Optical Techniques in Optogenetics

Article *in* Journal of Modern Optics · May 2015

DOI: 10.1080/09500340.2015.1010620

CITATIONS
61

READS
1,096

2 authors:

Samarendra Mohanty
University of Texas at Arlington
168 PUBLICATIONS **2,904** CITATIONS

SEE PROFILE

Vasudevan Lakshminarayanan
University of Waterloo
570 PUBLICATIONS **4,765** CITATIONS

SEE PROFILE

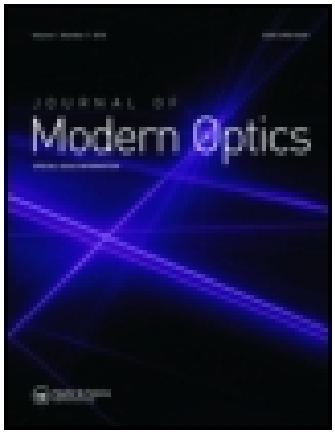

Journal of Modern Optics
Publication details, including instructions for authors and subscription information:
http://www.tandfonline.com/loi/tmop20

Optical techniques in optogenetics

Samarendra K. Mohanty[a] & Vasudevan Lakshminarayananan[bc]

[a] Department of Physics, Biophysics and Physiology Group, The University of Texas at Arlington, Arlington, TX, USA

[b] Department of Physics and Electrical and Computer Engineering, School of Optometry and Vision Science, University of Waterloo, Waterloo, Canada

[c] Department of Physics, Unviersity of Michigan, Ann Arbor, MI, USA

Published online: 12 May 2015.

Journal of Modern Optics, 2015
http://dx.doi.org/10.1080/09500340.2015.1010620

Taylor & Francis
Taylor & Francis Group

TUTORIAL REVIEW

Optical techniques in optogenetics

Samarendra K. Mohanty[a]* and Vasudevan Lakshminarayananan[b,c]

[a]*Department of Physics, Biophysics and Physiology Group, The University of Texas at Arlington, Arlington, TX, USA;* [b]*Department of Physics and Electrical and Computer Engineering, School of Optometry and Vision Science, University of Waterloo, Waterloo, Canada;* [c]*Department of Physics, Unviersity of Michigan, Ann Arbor, MI, USA*

(*Received 14 December 2014; accepted 14 January 2015*)

Optogenetics is an innovative technique for optical control of cells. This field has exploded over the past decade or so and has given rise to great advances in neuroscience. A variety of applications both from the basic and applied research have emerged, turning the early ideas into a powerful paradigm for cell biology, neuroscience, and medical research. This review aims at highlighting the basic concepts that are essential for a comprehensive understanding of optogenetics and some important biological/biomedical applications. Further, emphasis is placed on advancement in optogenetics-associated light-based methods for controlling gene expression, spatially controlled optogenetic stimulation and detection of cellular activities.

Keywords: optogenetics; neuroscience; cell biology; biomedical optics; biophysics; biophotonics; vision science

1. Introduction

The continued interest of scientists in the study and understanding of the heterogeneous living systems such as the brain has prompted new developments in microscopy. Optical tools have been used for genetic analysis and gene sequencing as well as for genetic manipulation and inserting genes into cells. Optics and genetics together has allowed for visualization of cellular structures (e.g. by fluorescent proteins) and functions (e.g. by genetically encoded voltage indicators (GEVI)). Use of photonics tools not only allows high-resolution imaging of structure and function of neurons, but also holds promise for manipulating neural circuits. Optical techniques such as glutamate uncaging have offered unique methods to manipulate cellular activity. However, optogenetic stimulation appears to be the most advantageous tool for the study and manipulation of cellular systems including neurons. Distinctive features that make this technique stand out from others include cellular specificity and high temporal resolution. Optogenetics present cell-specific control of activities using optics and genetics.

Several improvisations had to be made that finally made possible the expanded use of optogenetics. Discovery of light-sensitive ion channels (opsins) dates back to previous few decades (1970–1990). History of optogenetic activation is presented in Figure 1. A type of bacteria, *Halobacterium salinarum*, that lives in highly saline environments (>4 M salt), can live with light as the only energy source due to the activity of the retinal protein bacteriorhodopsin. Bacteriorhodopsin [1,2], a light-driven proton pump converts light energy into a proton gradient and the energy stored in the proton gradient is used in different ways, such as generation of Adenosine triPhosphate (ATP), the basic building block of energy in the living system. Besides bacteriorhodopsin, *H. salinarum* contains other retinal proteins (photosynthetic pigments with a retinal chromophore) including halorhodopsin [1,3]. Halorhodopsin is a light-driven chloride pump that permits *Halobacterium* to maintain high internal salt concentration upon growth. Organisms expressing these rhodopsins work in environments with high salt concentrations. Okuno et al. [4] demonstrated the use of halorhodopsins in a physiological environment. In contrast to *H. salinarum*, halorhodopsins from *Natronomona pharaonis* were functional at physiological chloride concentration level. However, in spite of their suitability for activating neurons, use of these halorhodopsins in neurons was not attempted for almost a decade. During this period, Gero Miesenbock and colleagues [5] created a 3-gene Drosophila phototransduction cascade (chARGe: Arrestin-2 rhodopsin coupled to α-subunit of G-protein) for activation of neurons. When exposed to light, chARGe-expressing neurons could be activated [5]. However, since the activation of neurons took several seconds, there was a need for a temporally precise method of activation. While light activation of light-sensitive protein ion channel (halorhodopsin) has been realized in late 1970s, it was not until the early 2000, when light activation of another opsin, channelrhodopsin was observed [6] to lead to fast and reliable transport of cations across cell membrane, that the concept of fast

*Corresponding author. Email: smohanty@uta.edu

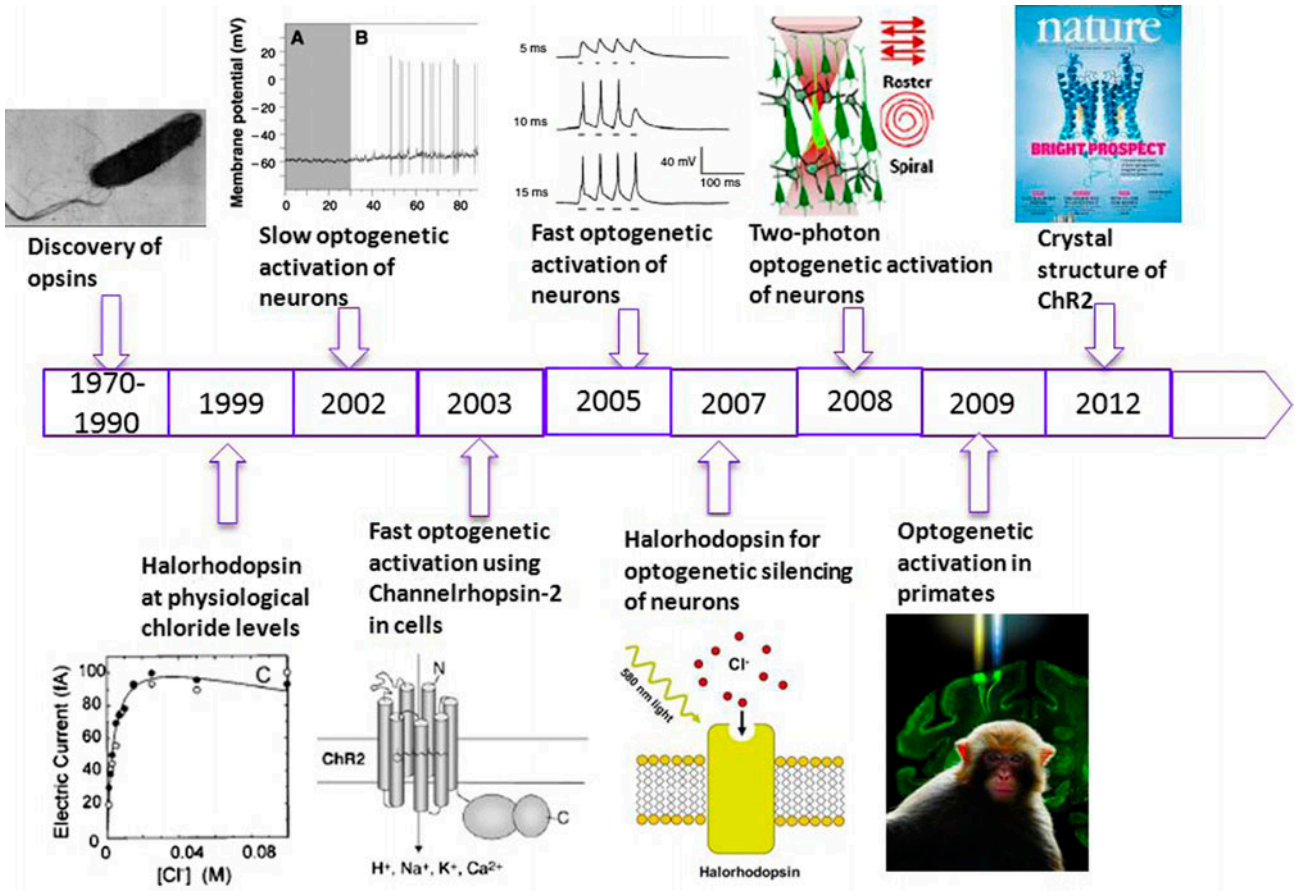

Figure 1. History of optogenetic activation. Insets: 1999 - Reprinted with permission from Ref. 4, Copyright 1999, American Chemical Society; 2002 - Reprinted with permission from Ref. 5; 2003 - Reprinted with permission from Ref. 6; 2005 - Reprinted with permission from Ref. 7; 2012 - Adapted from cover illustration for Ref. 20. (The color version of this figure is included in the online version of the journal.)

optogenetic stimulation was realized and reliable fast activation of neurons using light began to turn into a real possibility in 2005 [7,8].

The main purpose of this tutorial review is to give a picture of the field of optogenetics, especially focusing on optogenetic stimulation. This review does not pretend to be an exhaustive document but aims to give a view of the field from the viewpoint of optics. We will explain the basic mechanisms of optogenetics, followed by a description of tissue optics for understanding of propagation of stimulating light in neural tissue. Optical experimentation and applications of optogenetic stimulation for control of neural functions will be discussed next. Then, we will explore the possibilities of optogenetics-associated light-based methods for controlling gene expression and spatially controlled optogenetic stimulation. Finally, we will discuss optical detection of cellular activities during optogenetic stimulation and conclude with the challenges and future prospects in the field. Other reviews [9–15] may offer a different perspective or contain complementary material and further references on various other aspects of the field, and the interested reader is encouraged to go through those references.

2. Basics of optogenetic stimulation

In a broad sense, optogenetics refers to the use of optics and genetics together for controlling activity of proteins and cellular function or in other words, optical control of the functioning of genetically targeted/modified cells. The cellular functions that can be controlled with optogenetics include stimulation/inhibition of cells, gene activation, intracellular signaling, and migration. Types of cells that optogenetics can control include neurons, cardiac cells, stem cells, and cancer cells. However, since focus of this review is on optics, let's focus on controlling a particular function (i.e. stimulation/inhibition) of neuronal cells. Non-specific stimulation or inhibition of defined groups of neurons in brain or peripheral nervous system by conventional electrical and other non-optical methods has been a major hindrance for application of stimulation strategies for therapeutic purposes.

Furthermore, study of function of specific neurons in native circuitry needs precise control of activity, which requires dissection to allow accurate positioning of stimulating electrodes. Thus, it has been inherently difficult to perform non-optical (i.e. electrical, magnetic, etc.), (cell)-specific stimulation in live animals. Even with the ultrafast laser stimulation or the light-assisted glutamate uncaging, the problem with selective activation persists. Emerging methods that combine optics and genetics have scientists speculating about the possibilities of realizing a remote-controlled switch into the brain. The ingredients for realization of the optogenetic stimulation include four major steps as depicted pictorially in Figure 2.

2.1. *Light-activated proteins*

Out of many opsins (light-gated ion channels), channelrhodopsin-2 (ChR2) is an important photochemical switch responsible for phototaxic nature of algae *Chlamydomonas reinhardtii.* Eye spot of *C. reinhardtii* contains the 7-transmembrane-helix protein Channelrhodopsin-2 (a cation channel). ChR2 is activatable with ms-kinetics, in presence of chromophore all-trans-retinal (ATR), by a band of blue light ($\lambda = 440$–500 nm) with intensity threshold less than 1 mW/mm^2. Nagel et al. [6] first showed that ChR2 can be used to depolarize cells (HEK and oocytes) upon blue light illumination with high temporal precision. Two years later, *in vitro* optogenetic activation of neurons using ChR2 was demonstrated [7]. During the same year, optogenetic stimulation of chick spinal cord [16], behaving worm [8], and even intact mammalian brain circuits [17] was reported. In addition to stimulation, silencing of neurons (*in vitro* as well as *in vivo*) has been reported using chloride channel-based halorhodopsin (NpHR) [18,19]. Since the activation peak of halorhodopsin is in the yellow spectral range, well separated from the blue-activation peak of ChR2, multimodal optical stimulation and silencing of neural activity is possible using multiple wavelengths of light with high temporal resolution.

The first step involves synthesis of a genetic construct encoding the opsin. Since ChR2 opsin itself is not fluorescent, plasmid encoding for ChR2 (or other opsins) is fused with fluorescent reporter protein for visualizing their expression in cells. Further, for cell-specific stimulation, the opsin can be made to express in genetically targeted cells using promoter in the genetic construct. The crystal structure of a ChR (a C1C2 chimaera between ChR1 and ChR2 from *C. reinhardtii*) at 2.3 Å resolution has been recently reported [20]. To obtain better optical control (e.g. narrow activation spectrum, kinetics), and efficient transfection into cells, the opsin construct has been modified using genetic engineering. Mutations in the opsin construct has led to higher channel conductance, better light sensitivity (i.e. lower threshold intensity for stimulation), red-shifted spectral response [21], faster kinetics of the ion channel, ion selectivity [22], and higher expression level. For example, mutation of ChR2 leads to change in efficiency in generating photocurrent [20]. Furthermore, opsins derived from different organisms [23] have different photocurrent generation efficiency. For example, Archaerhodopsin (Arch), which hyperpolarizes the neuron by pumping out protons, could completely silence the neu-

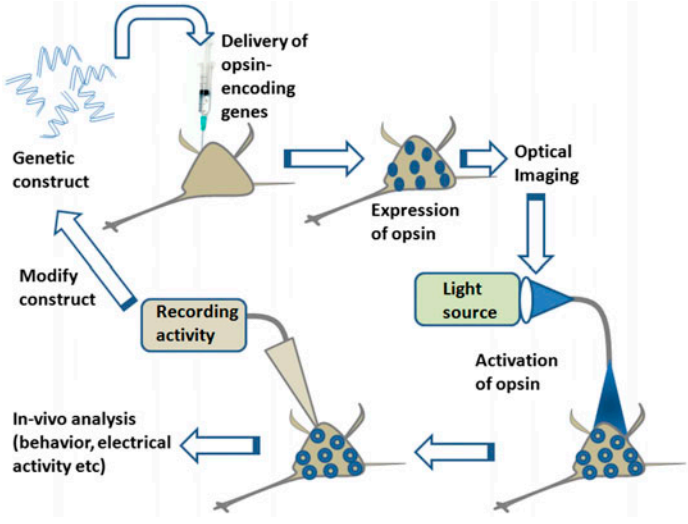

Figure 2. Intuitive description of optogenetic stimulation method. Synthesis of genetic construct encoding opsin, delivery and expression of opsin in targeted cells, optical activation of opsin-expressing cells, followed by readouts and modification of construct to obtain better optical control. (The color version of this figure is included in the online version of the journal.)

Table 1. Key components of major steps in optogenetics.

Light-activated proteins	Gene delivery and expression
• Intensity threshold • Wavelength selectivity • Kinetics • Current activity • Ion selectivity	• Virus-mediated delivery • Transgenic animals • Promoters • Conditional expression system • Non-viral delivery
Illumination	**Readout**
• Wavelength engineering • Temporal control • Focused vs. wide-field • Multi beam (digital micromirrors) • LED vs. fiber/arrays • Light propagation in tissue	• Electrodes/arrays • Fluorescence biosensors (dyes/genetically encoded) • Label-free detection • Behavior (cell/animal)

ron [23] (as compared to halorhodopsin [18,19]) due to its larger photocurrents and faster recovery after switching off the light. Table 1 below lists key components of the major steps of optogenetics activation.

For non-mammalian neurons or other cells co-factor ATR needs to be added few hours prior to the optogenetic activation. Since ATR is present in mammalian neurons, no external addition of the co-factor (ATR) is required for generating light-activated action potential.

2.2. Gene delivery and expression

The second major step in the optogenetic stimulation method comprises delivery of opsin-encoding plasmids into targeted cells integrated with expression analysis using (reporter) fluorescence imaging. Viral gene delivery provides a convenient and quick approach for mediating opsin expression. Generally, adeno-associated virus (AAV) or lentivirus is used to package the opsin construct and deliver near the neurons in Petri dish or into the brain region of interest. Lentiviral vectors are integrated into the genome of the target cell [24] and therefore, confer permanent gene expression. Viral vectors carrying the genes encoding ChR2 can be delivered stereotactically [25] into discrete brain regions [19,26]. AAV-mediated expression may be less stable because a much smaller percentage of the virus is integrated. These vectors can be rendered specific cell type by the choice of promoter [27], viral receptors [28], or spatial targeting strategies [29]. The volume and concentration of virus determine the spread in the tissue and opsin expression region. Besides viral method, non-viral expression of opsin has been achieved using lipofection, (*in utero*) electroporation, and optoporation (which we will discuss in detail later). Use of promoters or conditional expression system allows expression in a cell-specific manner. Further, transgenic animals expressing opsins in specific cell type, have been developed for optogenetic research, and are also available commercially (Jackson Laboratory).

Before transfecting the neurons, the plasmids encoding opsins are sometimes first tested for expression in model cells (HEK 293). For cells or neurons in monolayer (*in vitro*), the expression of the opsin in selected cells (or cell types) is confirmed by visualizing the fluorescent reporter protein using conventional epifluorescence microscope (Figure 3, top panel). In order to monitor the fluorescence in deep brain structures, fluorescence collected by an optical fiber (also carrying the fluorescence excitation laser beam) is separated by a dichroic mirror (DM), filtered by a band-pass emission filter (Em), and detected by a photo-detector (APD or PMT) as shown in bottom panel of Figure 3. *In vivo* expression imaging with single-cell resolution is possible by confocal (or multiphoton) microscopy with special arrangement (such as optical window on dura mater, with skull removed). However, for analyzing opsin expression in the deep brain regions with cellular resolution and to confirm expression in specific cell types, at the end of the *in vivo* experiments, the test animal is sacrificed and the brain is extracted and sliced using a microtome. For imaging opsin expression, the brain slices are visualized using confocal microscopy without requiring any additional staining. For correlating opsin expression with specific cell types, immunohistochemistry is carried out on the brain slices, which include fixing and staining of the slices by fluorescent antibodies specific to the opsin-reporter protein (one for each, e.g. ChR2-YFP, NpHR-RFP) and antibodies specific to specific cell types (e.g. tyrosine *hydroxylase* for dopaminergic cells). The co-localization between these fluorescent antibodies is imaged by confocal fluorescence microscopy.

2.3. Illumination

Different illumination parameters are used for controlled optical activation of opsin-expressing cells. The wavelength of the light source is tuned to maximum activation peak of the opsin. For simultaneous activation and

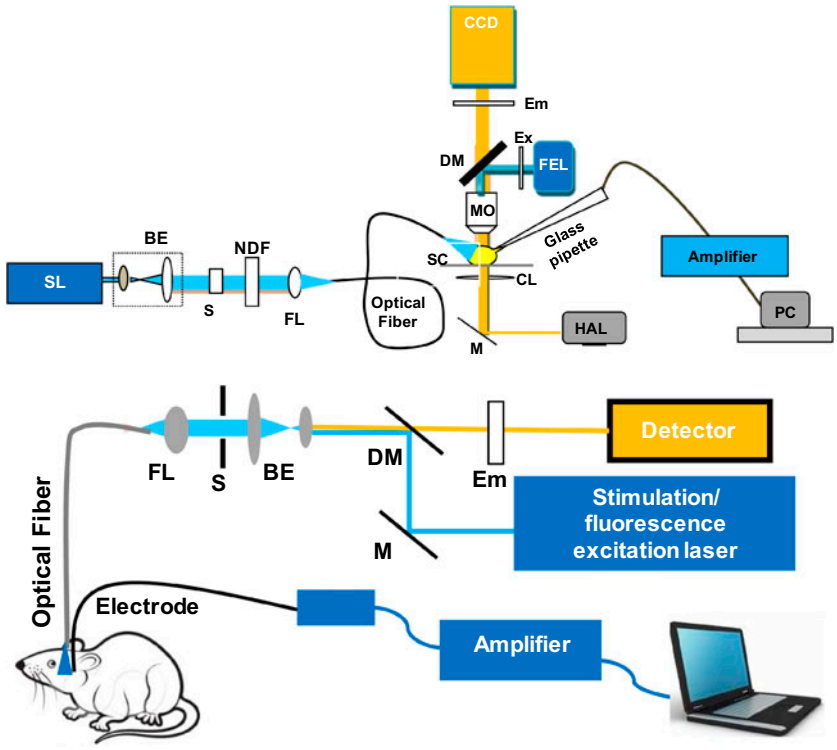

Figure 3. Typical experimental setups for optogenetic stimulation and characterization. Top: *in vitro* optogenetic stimulation setup integrated with patch clamp recording and optical imaging ability. SL: stimulation laser; BE: beam expander; S: shutter; NDF: neutral density filter; FL: focusing lens for coupling to optical fiber; FEL: fluorescence excitation lamp; Ex: excitation filter; DM: dichroic mirror; Em: emission filter; MO: microscope objective; SC: sample chamber; CL: condenser lens; M: mirror; HAL: halogen lamp. Bottom: setup for *in vivo* fiber-optic optogenetic stimulation, electrophysiological recording and optical detection. M: mirror; DM: dichroic mirror; Em: emission filter. (The color version of this figure is included in the online version of the journal.)

silencing of same neurons or two different neuronal populations, both channelrhodopsin-2 (activated by blue light) and halorhodopsin (activated by orange light) have to be expressed in the targeted neurons. This combinatorial optogenetics modulation of cells requires use of two different sources. The cells can be illuminated by the two light beams (blue and orange) emanating from two bright light-emitting diode (LED) sources, physically arranged (say side-by-side or at an angle) so as to overlap in the region of interest. The two beams having different wavelengths can be combined using a DM (in case of free-space arrangement) or fiber optically (e.g. in case of fiber-coupled LEDs). For controlling multiple sets of neurons expressing different opsins, multiple colors of activation light beams have to be multiplexed. Use of fast switching mechanism can allow sequential illumination with multiple wavelengths (with defined delay between any two beams).

Besides wavelength engineering, temporal control of light pulses (pulse width, gap between pulses, repetition rate) is required for controlling and probing neurons. This can be achieved using function generators controlling the drivers of the source (LEDs or diode lasers) directly or by controlling an external electro-mechanical shutter in the path of the stimulation light beam. For neuronal activation, periodic pulses having pulse width in the range of ~1–500 ms and frequency (repetition rate) in the range of 1–100 Hz are being used. The gap between the light pulses is decided by the frequency and duty cycle of the pulse's On vs. Off duration. Further, different non-periodic (e.g. Poisson-distributed) pulse patterns are generated via computer to optically modulate and probe neuronal function. The top panel of Figure 3 shows schematics of a typical laser-based optogenetic stimulation setup. In this case, the stimulation laser (SL) beam(s) is (are) first expanded using beam expander (BE) and shutter (S) is placed to control the temporal profile. A neutral density filter (NDF) is placed next to enable variation of stimulation intensity.

The intensity can also be controlled by other convenient means such as control of the driving currents (in case of LEDs) or use of rotating polarizer and half wave plate (in case of laser) or acousto-optic tunable filter. A focusing lens (FL) is used to couple the SL beam to an optical fiber (generally multimode having core diameter 50–200 μm) so as to allow easy positioning of the fiber

tip near the sample chamber (SC) or region of interest in brain (bottom panel of Figure 3) containing the opsin-sensitized neurons. Thus, wide-field stimulation of many opsin-sensitized neurons in the region of interest is possible using cleaved multimode optical fiber (Figure 4(*a*) and (*b*)), or even using spectrally filtered (by narrow-band excitation filter, Ex) light beam from the fluorescence excitation lamp (FEL) weakly focused by the microscope objective (MO) as shown in case of free-space setup (Top panel of Figure 3).

For controlling multiple sets of neurons expressing different opsins (e.g. ChR2 and C1V1), multiple colors of activation light beams (e.g. blue and green) can be coupled to the same fiber and delivered to the region of interest as shown in Figure 4(*c*). However, certain applications require stimulation/inhibition of a single neuron (within the specific group of one cell type). In such cases, laser (instead of lamp) beam can be focused using a lens resulting in spot size of (1.22 λ/numerical aperture (NA)). Thus, for $\lambda = 473$ nm, and NA of 0.15, the diffraction limited spot size is ~4 μm, which is smaller than size of the soma of a neuron. Figure 4(*d*) shows single neuronal stimulation using focused blue light. While focused visible laser beams are very well suited for spatially localized optogenetic activation of cells in two-dimensional transverse plane, the out-of-focus visible light is sufficient to stimulate other opsin-sensitized cells, reducing the axial resolution. Better axially localized stimulation can be achieved by controlling the intensity of the visible stimulation light so that the intensity at the focal volume (Rayleigh range) is just above the threshold of the opsin activation. It may be noted that to achieve higher axial activation resolution, two-photon optogenetic stimulation of cells could be achieved using ultrafast (femtosecond (fs)) near-infrared (NIR) laser beam. The higher axial resolution is due to the non-linear nature of light–opsin interaction in case of ultrafast laser beam in contrast to the linear nature of interaction between the visible light and opsin. We will discuss this in detail later in this article.

Different illumination strategies for optogenetic activation are summarized in Figure 4. For activation of multiple (selected) opsin-sensitized cells simultaneously, or in a temporally controlled pattern with single-cell resolution (Figure 4(*e*)), multiple focused activation beams have to be generated and controlled. This can be achieved using time-sharing beams generated by acousto-optic deflector or scanning mirrors. However, since the scanning in such case will be limited by the dwell time, faster or better temporal control of activation can be achieved using digital micromirror device or spatial light modulator. Further, arrays of independently controllable CMOS-driven μLEDs with a pitch of <100 μm have been created for spatio-temporal control on optogenetic stimulation [30,31]. The multiple beams generated

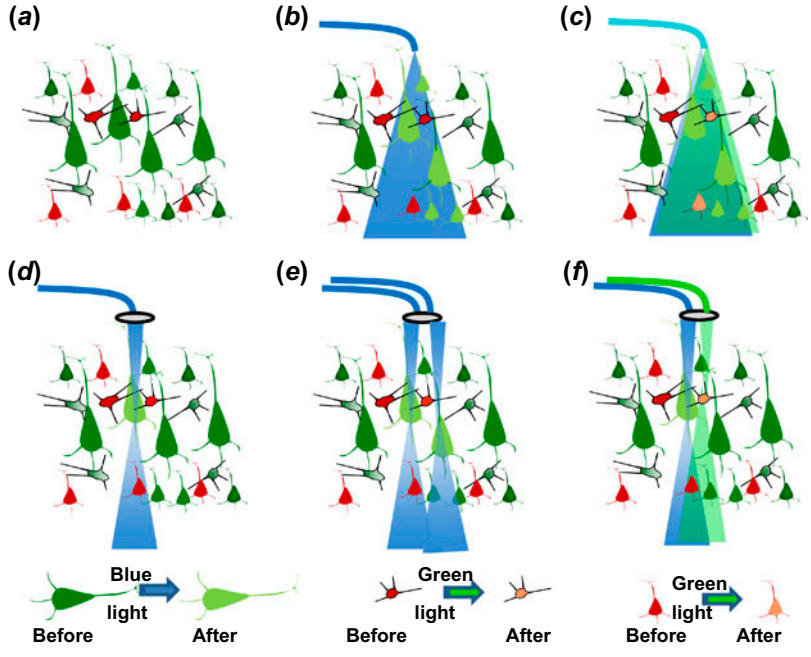

Figure 4. Different illumination strategies for optogenetic activation. (*a*) Different cell types sensitized by different color opsins. (*b*) Activation of one (green) cell type using wide-field blue activation beam. (*c*) Activation of two (green and red) cell types using wavelength multiplexed beams (blue & green). (*d*) Activation of one (green) cell using focused blue activation beam. (*e*) Activation of multiple (green) cells using multiple blue activation beams. (*f*) Activation of one (green) and another (red) cell using focused blue and green activation beams. (The color version of this figure is included in the online version of the journal.)

by either of the above methods can be coupled to the microscope for *in vitro* optogenetic activation or to arrays of optical fibers for *in vivo* applications. In order to control activation of selected (multiple) cells sensitized by different opsins, it is necessary to be able to generate multiple laser beams of different colors and control them individually (Figure 4(*f*)).

Visible light is significantly scattered in tissue (including brain) by cellular structures leading to diffused light as the beam propagates through the tissue. Therefore, use of adaptive optics and other phase correction measures need to be implemented for maintaining the spatial profile of the optogenetic activation beam at depth. In addition to large scattering, significant absorption by cellular chromophores leads to attenuation of visible light in tissue. Therefore, delivery of visible stimulation light to deep brain regions requires use of waveguide(s) or insertion of the μLED source(s) in the brain. Optical fibers of different diameters (50–200 μm) as well as integrated optical waveguides have been used to carry the stimulation light in to the brain regions (Figure 3, bottom). For keeping the waveguide/fiber in place inside brain during *in vivo* experiments, it is held using a stereotaxic unit in case of anesthetized animals. However, for experiments in freely moving animals, a cannula guide is pre-fixed to the skull (by screws or dental cement) of the animal, through which the optical fiber is inserted and fixed. An optical commutator (connecting one end to the fiber from the source and other end to the fiber fixed with the cannula) is used in order to allow free movement of the animal and avoid breakage of the optical fiber during experiment.

2.4. Readout

The gold standard of neural electrophysiological recordings has been, and still is, electrode-based recording (the patch clamp method). To measure intracellular current or generation/inhibition of action potential by light activation, patch clamp recordings in voltage clamp and /or current clamp mode are generally carried out *in vitro* (though it can be carried out *in vivo* as well). Patch clamp works by applying light suction to a cell membrane via a glass or quartz pipette containing a single conductive electrode. The applied suction creates a high-resistance seal between the membrane and the pipette sometimes referred to as a 'gigaseal' due to the resistance of this seal often being on the order of gigaOhms. This high-resistance seal allows for extremely small (pico-) currents to be measured by the electrode and amplifier equipment. A typical opto-electrophysiology setup is shown in top panel of Figure 3. Both upright and inverted microscope platform can be used for patch clamp recording. For whole-cell patch clamp, borosilicate micropipettes of resistance in the range of 3–5 MΩ are made using pipette puller. The micropipette is filled with an intracellular solution containing (in mM) 130 K-Gluconate, 7 KCl, 2 NaCl, 1 $MgCl_2$, 0.4 EGTA, 10 HEPES, 2 ATP-Mg, 0.3 GTP-Tris, and 20 sucrose. The micropipette electrode is mounted on an XYZ micromanipulator to position the electrode on the cell (of interest) being illuminated by stimulation beam. The signal from cell (upon light stimulation) is amplified and the output from the amplifier is digitized and recorded with patch clamp software. The physiological environment (e.g. temperature and CO_2) of the cells is maintained and the whole system needs to be isolated from vibration (using vibration isolation table). Electrical isolation is achieved by placing a Faraday-cage around the setup. For electrophysiological measurements subsequent to optical activation, the light pulses (generated internally, or by use of external shutter) need to be synchronized with the patch clamp recording. This allows measurement of delay between the activation pulse and peak current (or voltage) and quantification of jitter etc.

Further, to detect stimulation/inhibition of neurons by optogenetic activation, *in vitro* (and *in vivo*) single metallic (e.g. tungsten) electrode as well as array containing multiple electrodes is used. For *in vitro* measurements, planar electrode(s) is (are) fabricated for culturing neurons on them. Two-dimensional array of slanted electrodes or linear array (reaching different depths in brain) is used for *in vivo* electrical recording of optogenetic modulation of neural circuits. In special cases, electrode has been integrated with fiber so that separation between electrode and fiber can be varied. Otherwise, electrodes are fabricated with fixed separation from the fiber/waveguide delivering the stimulation/inhibition light. Such multifunctional device is called optrode. Optrode has also been made with light source (μLED) integrated with the recording electrodes, which can be inserted into the brain for simultaneous optogenetic stimulation and recording. When free movement of animal is required during optogenetic stimulation and electrical recording, electrical commutator can be used to avoid twisting of electrical connections. Using wireless technologies, such mechanical considerations for recording can be eliminated. In cases where free movement during recording is not required, animals are deeply anesthetized (e.g. with 90 mg/kg ketamine and 10 mg/kg xylazine) and placed in a stereotaxic frame. In these type of *in vivo* recording from brain of anesthetized animal, linear midline skin incision is made and burr hole is drilled in the skull at the desired anteroposterior (in reference to Bregma) and mediolateral coordinates corresponding to the brain region of interest. The electrode is then positioned stereotaxically to allow recording from deep brain regions. Figure 5 shows a representative in-depth electrical recording of neural activities in response to fiber-optic optogenetic stimulation in Thy1-ChR2 transgenic mouse

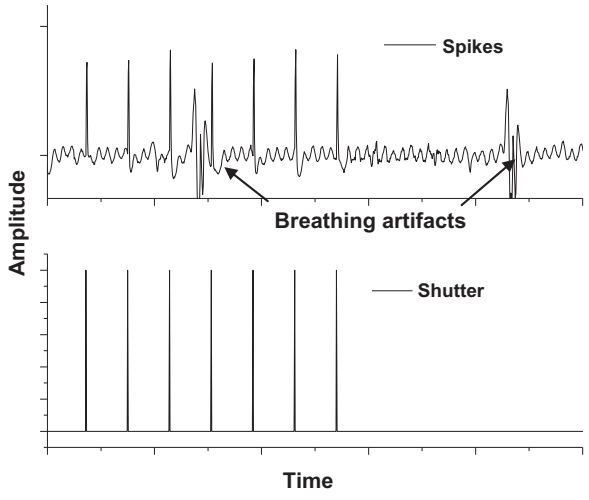

Figure 5. In-depth electrical recording of neural activities in response to fiber-optic optogenetic stimulation. Spiking activities (top) in Thy1-ChR2 transgenic mouse brain in response to optogenetic stimulation pulses (bottom), controlled by electro-mechanical shutter. The breathing artifacts in recorded signal can be seen.

brain. Electrical recordings provide measure of several parameters such as induced current, light-evoked potential, firing/spike rate and inter spike interval (ISI). Further data processing such as quantification of channel kinetics (in case of patch clamp recording), and spike sorting (in case of *in vivo* recordings) can be carried out using advanced commercial softwares.

Fluorescence biosensors such as calcium dyes (e.g. Fura, Calcium Orange, Fluo-3) are also used for monitoring neural activities and its optical modulation. To improve the temporal resolution of optical monitoring of neural activities, GEVI having faster kinetics are being used recently. Multiphoton microscopy has been utilized to image neural activities and their modulation in tissue slices as well as in superficial layers of brain *in vivo*. In that case, the mirror (M) in bottom panel of Figure 3 is replaced by a scanning mirror. In order to monitor the calcium fluorescence in deep brain structures, fluorescence collected by an optical fiber/array (also carrying the fluorescence excitation laser beam) can be separated by a DM, filtered by a band-pass Em, and detected by a photo-detector (APD/PMT or CCD) as shown in bottom panel of Figure 3. In order to allow free movement of the animal and avoid breakage of the optical detection fiber during experiment, fiber-optical commutator is recommended. To avoid photobleaching and cytotoxicity in case of fluorescence dyes and to avoid use of additional gene-delivery expression for monitoring neural activities as well as to improve temporal resolution, label-free optical detection of neural activities is recently attempted which will be discussed in a later section. While all of the above recording methods are very crucial for evaluating neural activation by optogenetic stimulation/inhibition; monitoring the behavior (e.g. movement) of animal (whose brain region is being modulated) provides another critical measure for evaluating overall outcome of the optogenetic manipulation. Based on the read out values (inward current, evoked potential, etc.), the optogenetic construct can be modified and/or illumination parameters (wavelength, pulse width, intensity, etc.) can be optimized to obtain better optical control of targeted neurons and overall function of the neural circuitry.

3. Light propagation in tissue

For success of most of the key steps in optogenetics method, starting from *in vivo* visualization of opsin expression, to optical activation of opsin-expressing cells and optical detection of neural activities, understanding of propagation of light in tissue is very important. Attenuation in light through neural tissue occurs due to absorption by tissue chromophore and multiple scattering by the tissue microstructure. This attenuation is very high in the brain as the wavelength of light decreases. The attenuation of intensity of light of particular wavelength can be simulated using absorption and scattering properties (μ_a: absorption coefficient; μ_s: scattering coefficient) of the tissue at that wavelength. The light intensity (I_0) in tissue (I) is known to decay as a function of tissue depth or thickness (t): $I = I_0[e^{-\mu_{eff}t}]$, where μ_{eff}, the effective attenuation coefficient is given by sqrt $[3\mu_a(\mu_a+\mu_s')]$; and μ_s' is the reduced scattering coefficient, given by $\mu_s(1-g)$, g being the anisotropy factor of the forward scattering tissue.

Figure 6 shows theoretically calculated variation of light intensity (I) as a function of brain (white matter) depth (t) for known absorption and scattering properties at 480 nm (Table 2). As can be seen from the graph, after traveling through a depth of 1 mm, the blue laser beam gets attenuated by 90%. This intensity decay is less drastic when lights with red-shifted wavelengths are used for imaging of expression, or stimulation of targeted neurons, or detection of neural activities. With use of visible light beam, neurons at larger depths can be reached by increasing the power of the incident laser beam. However, as a word of caution, this approach will lead to significant detrimental effects on the viability of neurons closer to the source, especially for long-term stimulation studies. It may also be noted that the spatial resolution of focused illumination strategies for optogenetic activation (Figure 4) will be largely compromised due to the significant diffusion of light as the tissue depth increases. However, phase conjugation methods (by adaptive optics) may be employed to restrict the distortion of spatial profile of the laser beam and thus obtain better spatial precision. Since the brain is a

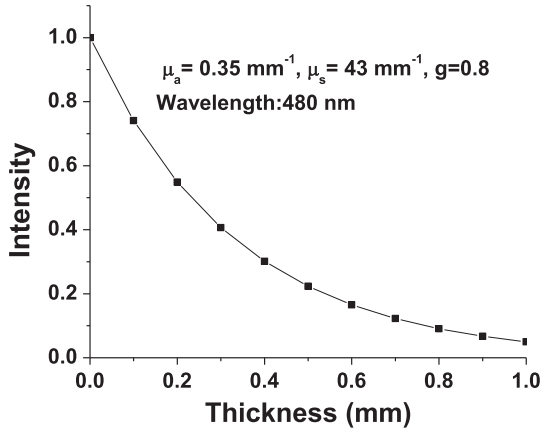

Figure 6. Calculated attenuation of intensity as a function of tissue depth or thickness. White matter tissue optical properties at 480 nm are listed.

heterogeneous media with multiple layers of tissues having different thickness and optical properties, it is essential to model light propagation more accurately.

3.1. *Monte Carlo simulation*

Monte Carlo (MC) simulation is considered as the most reliable method for modeling photon migration in such heterogeneous conditions. It becomes even more important when it is required to model laser beam emanating from fiber (or via lens) having different NA and for beams having different shapes. For Monte Carlo simulations, the widely used MCML software [32], targeted for multilayered media, can be used. For Gaussian beam launching, using a random number evenly distributed between 0 and 1, the relationship can be determined among the random number and a launch radius, following a Gaussian probability density function with $1/e$ intensity radius. NA affects the launching direction of photons using random number to choose angle referring to related relationship involving the error function [33]. Using the widely used Monte Carlo simulation codes for light propagation in multilayered biological tissue named 'MCML' [34] and 'COV' [35], the brain can be modeled as two-layered tissue including gray matter and white matter.

The absorption coefficient (μ_a), scattering coefficient (μ_s), anisotropy factor (g), refractive index (n), and thickness of cortical layers (t) parameters [36–38] can be set up at the light wavelength of interest for the simulation, and then light propagation with the MCML code can be computed. The paired code 'COV' can be utilized next to extract the simulation output and calibrate the computed fluence rate distribution by quantitatively carrying the effect of Gaussian beam distribution and respective parameters, including beam size, laser power, and NA. Figure 7 shows XZ-distribution of power density at different depths obtained using MC simulation of light propagation in two-layered cortex for two different wavelengths. As noticed, the orange (590 nm) light can reach greater depth than the blue (480 nm) light beam.

The limited/shallow penetration of the visible light has put some hindrance in classifying optogenetics as a minimally invasive method. Thus, in order to stimulate neurons which reside in the most ventral regions of the brain, one has to choose between one of two undesirable alternatives: the first alternative maintains the minimally mechanical-invasive qualities of the approach and requires that the average power of the light beam be significantly increased. Unfortunately, this approach has detrimental effects on the viability of neurons in the vicinity of the target. The second alternative is to use injectable μLEDs [39,40], or optical fiber-based delivery. This approach compromises the minimal invasive qualities of the technique because optical fibers (similar to electrodes used for electrical stimulation) need to penetrate through more superficial brain structures in order to reach more ventral brain regions. In this way, the more superficial brain areas get damaged and such damage may lead to difficulty in interpretation of the results of these experiments. The development of red-activatable opsin [21] has now opened new possibilities to stimulate brain regions at larger depths.

4. Applications

The advent of neuronal stimulation using optogenetics [41,42] has enabled highly selective activation of specific neurons with millisecond temporal precision. In contrast to electrical stimulation and treatment, optogenetics is

Table 2. Optical properties of the two-layered mouse brain model.

Wavelength (nm)	Layer	μ_a (mm^{-1})	μ_s (mm^{-1})	g	n	t (mm)
480	Gray matter	0.37	11.0	0.89	1.37	0.5
	White matter	0.35	43.0	0.8	1.37	2.5
590	Gray matter	0.19	9.7	0.89	1.36	0.5
	White matter	0.19	41.0	0.83	1.38	2.5

Note: μ_a = absorption coefficient; μ_s = scattering coefficient; g = anisotropy factor; n = refractive index, and t = thickness of cortical layers.

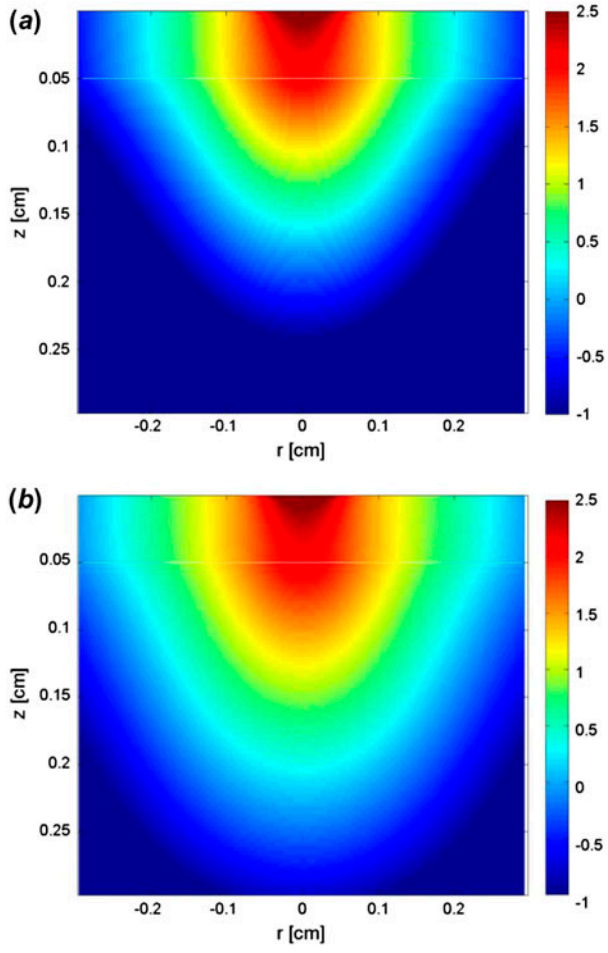

Figure 7. Monte Carlo (MC) simulation of propagation of light emanating from an optical fiber in two-layered cortex. XZ-distribution of power density (W/cm^2) in logarithmic unit is shown for (*a*) blue (480 nm) as well as (*b*) orange (590 nm) wavelengths. The NA of optical fiber is 0.22, and the beam diameter is 500 µm. The optical properties used for simulation of beams in the blue, and orange wavelengths [36,37] and tissue depths are listed in Table 1. 10^7 photons are launched in each simulation to achieve an excellent signal-to-noise ratio in simulation output [34,35]. (The color version of this figure is included in the online version of the journal.)

more specific and multiple types of neurons can be targeted at the same region of nervous system [43,44]. Optical stimulations, in general, are less susceptible to contamination and the requirement of mechanical stability is less stringent. This light-assisted method has higher spatial resolution (single-cell or subcellular level) as well as high throughput (parallel stimulation of multiple cells, wide area) and eliminates the highly challenging requirement of placing electrodes inside every single neuron of a specific type. Further, electrical noise reduction is only required during (and in cases of) electrical recording and not for stimulation (unlike electrical stimulation). Selective activation and silencing of neurons by ms light pulses have been demonstrated in cell culture [42,45], brain slices [46], as well as in small animals [47] sensitized with opsins. These light-sensitive opsins require very low-intensity (~mW/mm^2) illumination that can be delivered even from µLED [48]. Thus, optogenetics is emerging as a valuable experimental tool and a promising approach for intervening variety of disorders such as blindness [49–51], drug addiction [52,53], conditioned fear [54], epilepsy, pain, and Parkinson's disease [55] in animal models. Here, due to limitation of space, only one application (vision restoration) will be described to depict the use of optics in various ways.

Retinitis pigmentosa (RP) refers to blindness caused by degeneration of photoreceptors in the eye, which hinders visual function by non-functional neuronal activation and transmission of signals to the visual cortex [56–59]. RP is most often inherited as an autosomal recessive trait with large number of cases having this form of inheritance [56,58]. Although genetic testing is available for RP, it may not be sufficient to assess the risk of passing the disorder from parent to offspring, and even proactive approaches may not be sufficient to prevent its occurrence [56,59]. Further, the degree of visual loss increases with aging and this is a major concern because of demographic changes resulting in an elderly population. Most of the current clinical treatments are primarily focused on slowing down the progression of the disease [60], as there is neither any cure that can stop the disease nor any therapy that can restore any vision lost due to this disease [61]. The current treatment modality for partial restoration of vision for RP patients involves invasive surgical procedure for retinal implants based on electrical stimulation. Two different types of retinal stimulation implants are being developed: subretinal [62–64] and epiretinal implants [65,66]. Recently, a company called Second Sight (Chicago, IL.) got FDA approval for treatment of RP using these implants. Besides being invasive in nature, these methods for restoration of vision in blind patients are based on non-specific cellular activation and have low spatial resolution due to low number of electrodes (higher number or density of electrodes requires more power, leading to damage of neural tissue by heat) [65,67]. Stimulation of retinal neuronal cells using optogenetics via use of channelrhodopsin-2 (ChR2) and blue light has opened up a new direction for restoration of vision with respect to treatment of RP. Recent studies on optogenetic means of vision restoration have used non-specific transfection of retina as well as promoter-specific targeting of retinal ganglion cells (RGCs), [51,68–71] and ON-bipolar cells [72] led to improvement of visual function. Further, silencing (or inhibition) longer persisting cone photoreceptors by light activation of chloride-channel opsin (Halorhodopsin) have shown new promise for therapeutic intervention for restoration of vision [72].

Both viral [69] and non-viral (electroporation [73]) delivery methods have been successfully employed to transfect opsins into higher order neurons in photodegenerated retina of blind mouse and rat models. *rd*1 and *rd*10 are two different blind mice models that have been used for optogenetic vision restoration, which shows different rate of photodegeneration (*rd*1: fast vs. r*d*10: slow). In both viral and non-viral delivery methods, ChR2-plasmid with Thy1 promoter is used to target RGCs, mGluR6 is used to specifically express ChR2 in ON-bipolar cells. Fluorescence reporter protein (e.g. EYFP) is fused in the ChR2-construct for visualization of opsin expression in targeted cells. For delivery of opsin constructs (either virally or by electroporation), mice are anesthetized and a sharpened tip of a sterilized microsyringe was inserted through the sclera into the vitreous cavity. The optimal transfection parameters (volume and concentration of plasmids/virus) need to be determined by quantifying the efficiency (% of transfected cells and reporter fluorescence expression intensity) and viability of retina.

To test functional activation of retina *in vitro* electrophysiology by patch clamp or multielectrode array (MEA) recordings are carried out. Further, to confirm activation of opsin-sensitized degenerated retina and transmission of signals to the cortex, measurements of visual light-evoked potential can be performed [74] *in vivo* in visual cortex using MEA. Figure 8 shows a typical spatial pattern of *in vivo* spiking map in primary visual cortex (measured by MEA) subsequent to stimulation of the Thy1-ChR2-YFP-expressing RGCs (in mouse eye) by blue LED. Since the blue light from the LED was not focused to a single RGC in retina, several electrodes responded to light stimulation, though spatial variation of spiking activities can be observed. The incident light intensity and frequency can be modulated, and the change in evoked potential (e.g. spike rate, ISI) can be measured in the different electrode recording channels to determine optimal parameters for development of optogenetics prosthetics, such as threshold light intensity for stimulation.

In addition to delivery of opsins to specific retinal layers by genetic engineering, threshold intensity level of stimulation light needs to be delivered onto the retina (through multirefractive structures of eye) *in vivo* for generating action potential and successful behavioral outcome. Therefore, success of optogenetic prosthetic development requires optical engineering considerations. Optical system design software can be used to model the non-image-forming light response for a dark-adapted pupil determining minimal source irradiance requirements to achieve sufficient intensity at retina for excitation of opsin. The parameters such as the stimulating source positioning in front of eye and divergence of the light can be determined for optimal light delivery to the retina. Multiple surfaces, namely, anterior and posterior corneal surfaces, aqueous humor, anterior and posterior lens surfaces, vitreous humor, and the retina, as well as aperture stops (e.g. pupil) can be defined for physical optics propagation method. Each surface has to be defined by the parameters: (i) the radius of curvature, (ii) thickness (axial distance of each of the surface from the previous surface), (iii) semi-diameter (being the radial thickness), and (iv) refractive index. The spot diagrams and the irradiance map at the retina can be obtained by such ray propagation method. For the light intensity at the retina to be above the opsin-stimulation threshold, the light source should have sufficient brightness and optimal divergence so that maximum light can be collected and focused by the cornea lens on to the retina. Unlike highly packed pigments in photoreceptors of intact retina which amplifies the signal in cascade, cells expressing opsin only on membrane would require orders of magnitude higher light intensity to elicit action potentials. The required photon flux to achieve this depends on the level of opsin expression. From the threshold irradiance at cell required for generating action potential while using specific opsin and the transmission

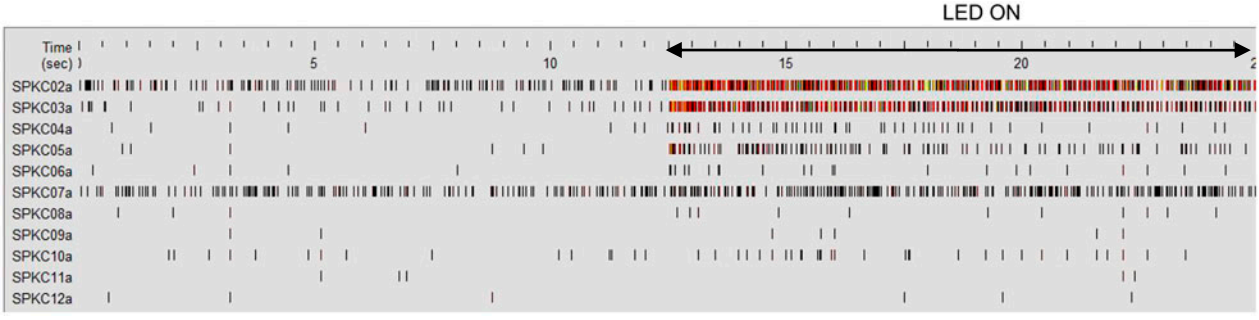

Figure 8. Light-evoked spiking activities in visual cortex of mice having optogenetically sensitized RGCs. A typical spatial pattern of *in vivo* spiking activities measured by MEA (16 channels, separated by 250 μm) in visual cortex (V1) subsequent to stimulation of the Thy1-ChR2-YFP expressing eye by blue (473 nm) LEDs. SPKC02a to12a denote different electrode channels in MEA. (The color version of this figure is included in the online version of the journal.)

characteristics of the eye, one can estimate the required radiance of the external light source to-be-used for development of optogenetic vision-restoration prosthesis. The source size, its position from the cornea and divergence need to be optimized for getting optimal modulation transfer function of the imaging system (eye). Besides these parameters, the spatial resolution of the optogenetically restored vision will depend primarily on the density of opsin-transfected neuronal cell type. Therefore, spatial resolution will be lower than achieved by the normal retina with tightly packed natural photoreceptors. Further, it may be comprehended that targeting of higher order neurons with low density such as RGCs may provide lower spatial resolution. However, excitation sensitivity of different regions (soma, axon) of one cell and respective processing of the information will contribute to the spatial resolution.

In order to determine restoration of vision by optogenetic stimulation, different behavioral tests can be conducted to evaluate different aspects of vision. For example, water maze test involves determination of score for the mice swimming toward a stimulating light source (on a platform) before and after optogenetic treatment. It provides a measure of directional light sensitivity. While this is an important measure, depth perception and pattern recognition are critical milestones that may also need to be evaluated to confirm behavioral restoration of vision by opsin sensitization. To evaluate improvement in depth perception, visual cliff experiment is carried out, wherein the animal (before and after opsin sensitization of retina) is made to walk on clear platforms above a checkerboard pattern that appeared to drop off abruptly. Untreated blind animals are expected to walk over either end of the platform, whereas animals with gained depth perception (by opsin sensitization) are likely to avoid the 'deep' end. For evaluating improvement of optomotor response in RP animal models having opsin-sensitized retina, the animal is placed on a platform surrounded by rotating vertical stripes and functional recovery of vision is evaluated via head tracking response. The basic principle of this analysis is the following: whenever a moving pattern is presented to an animal with normal vision, the animal will move its head to maintain stable vision of the pattern. If the animal possesses normal vision, it will move its head along with the movement of the vertical stripes. If the vision of the animal is poor, the animal will not show head movements in response to the moving pattern. The advantage of this method is that it does not require any previous training of the animal. All these behavioral assays for directional sensitivity, depth perception, and pattern recognition can be measured at different time points after opsin expression in retina. Figure 9 shows that mice transfected with ChR2 in eyes performed much better, in response to blue light source, than mice without

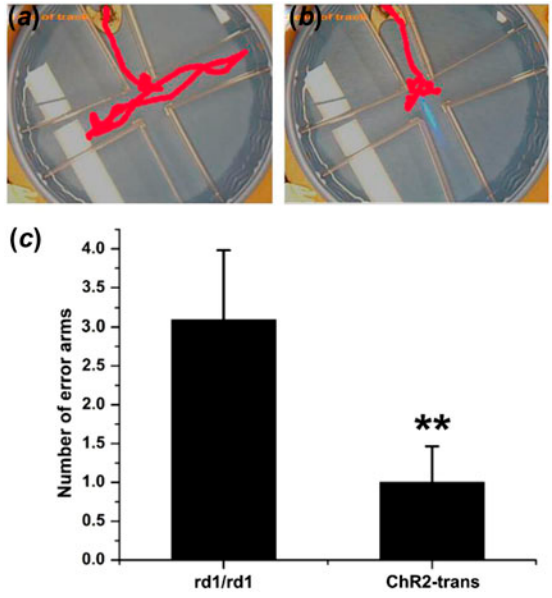

Figure 9. Water–maze assay of optogenetic vision restoration in mice having photodegenerated retina. Representative track of *rd*1/*rd*1 mouse (*a*) without and (*b*) with Thy1-ChR2 transfected retina. (*c*) Numbers of error arms mice swam before arriving at the platform (removable and suspended into the maze, filled with water). A weakly diverging light beam was directed into center of the maze. (The color version of this figure is included in the online version of the journal.)

transfection. As shown in Figure 9(*c*), the mean number of arms swam by the transfected mice before they reached the platform is significantly smaller than that of the mice without transfection. Commercial software is available to analyze the behavior of mice and to score based on swimming distance, swimming duration, and number of error arms traveled before finding the platform (light source) for evaluating the ability of the mouse to sense and respond to light of different characteristics (e.g. wavelengths, intensities, and divergence).

CMOS-controlled μLED array are being developed toward realization of optogenetics vision restoration. Similar to 'Second Sight' electrical stimulation approach, a camera-driven μLED array may further advance the resolution of restored vision. However, development of more efficient opsins and their targeted delivery needs to be developed for treatment of RP, where progressive loss of vision occurs from periphery toward center. Though we described above the development of optogenetics for vision restoration, the translation of technology for other applications is equal if not more challenging. Still, researchers are advancing the optogenetic applications in primate brains, taking a step closer toward possible clinical use. Han et al. [75] reported optogenetic activation in primate brains, where activity of specific subsets of neurons could be controlled, without causing immune responses and detectable cell death. Other groups have

shown use of different opsins for stimulation and silencing of neural activities in primates. The following sections will describe how optics and optical methods can complement conventional gene delivery, optogenetic stimulation, and neural activity detection methods.

5. Light-assisted opsin expression

While genes can be delivered by viral vector to all the neurons in a region (but with controlled expression using promoters), delivery to spatially targeted specific neurons requires microinjection by mechanical needles or microelectroporation, which pose significant challenge for *in vivo* applications besides damage to the neurons. Similarly, chemical methods including lipofection are not specific to targeted cells in a tissue and transfection efficiency of these methods varies depending on cell type and handling procedure. In last two decades, laser-assisted cellular poration (also called as photoporation, optoporation, or laserfection) has been utilized to efficiently introduce macromolecules into intact cells. Using a tightly focused laser beam, the cell membrane can be perforated in a highly controlled manner, allowing exogenous molecules to enter the cell. Since diffraction-limited spot size of UV laser beam is smaller and absorption of cell membrane is higher compared to longer wavelengths, lasers in the UV spectral range were the first to be used for microinjection [76]. However, UV light raises the potential of collateral damage to cellular components or even foreign DNA being transferred into cells [76], therefore, may not be suitable for non-invasive microinjection. Recently, there is considerable interest in optically transfecting cells using ultrafast-pulsed light [77–91] because of its selective targeting capability and higher efficiency and viability (>90% reported *in vitro* [77,90]) as compared to other methods. Further, fs NIR laser-based transfection has been shown to be safe, providing high efficiency and survival (93%) of optoporated embryo during development [92], as well as for *in vivo* gene delivery [93] as opposed to electroporation. Owing to the fact that absorption of cellular components are least in the NIR biological window of 700–1000 nm [81,94–96], recently NIR ultrafast laser beam was employed for laser-assisted poration. Because of highly localized damage by non-linear optical absorption, which fades away significantly for out-of-focus cellular components, fs laser beam could microinject exogenous genes into cells with very high efficiency [77,97,98]. The ultrahigh intensity as exists in a tightly focused fs-pulsed laser beam resulted in the formation of a site specific, transient perforation [77], more precisely than nanosecond-pulsed laser beam.

Efficient, non-contact and targeted delivery into specific cells can be achieved by NIR ultrafast laser microbeam by transiently puncturing the cell membrane, through which exogenous opsin genes can be microinjected with minimal damage. Use of ultrafast (~200 fs) NIR laser microbeam (800 nm, 76 MHz) for spatially localized transfection of retina with ChR2-YFP plasmids has recently been demonstrated (Figure 10) [78]. For transfection of specific area or volume, the focused NIR ultrafast laser beam is scanned over the region of interest by XY-scanning mirrors (e.g. galvanometric mirrors). The power of the laser microbeam, exposure (by an electro-mechanical shutter) at each focused spot and number of focused spots in the region of interest has to be varied in order to optimize laser transfection. This optoporation method using ultrafast-pulsed light provides selective targeting capability and high transfection efficiency and cell viability. Optoporation of ChR2 genes into targeted spatial location of retina explant as demonstrated with ultrafast laser microbeam may be extended for *in vivo* application in order to restore peripheral vision lost in RP. The success of the proposed optoporation studies will eliminate the requirement of viral delivery, which is disadvantageous in certain cases. For example, unlike adenoviral vectors, which are unable to substantially reinduce transgene expression by reinjection in rodents [99], it is desirable to reinduce transgene expression in neural tissue by reinjection, and optoporation provides this opportunity.

For optogenetic therapy applications, site-specific gene delivery is particularly important in order to avoid gene expression in non-targeted sites. Since optoporation method of opsin delivery is highly localized in region of application of optical field, risk associated with expression in non-targeted tissue is negligible. Besides use of fs laser microbeam, it is possible to use low-power continuous wave (CW) NIR laser beam along with photothermal agents for delivery of opsin plasmids into targeted cells [100]. Irradiation of the photothermal agents (e.g. carbon nanostructures) near the desired cell (s) with NIR laser beam leads to temperature rise that not only stretch the cell membrane to ease delivery, it also creates fluid flow to allow mobilization of opsin genes to the delivery site. Use of photothermal agents having significant absorption properties in the NIR therapeutic window will allow photothermal delivery (PTD) and targeted opsin expression under in vivo conditions (Figure 11).

Besides use of ultrafast NIR laser microbeam or photothermal agent-mediated delivery by CW NIR laser beam, optogenetic activation of specific light activatable proteins can be used to allow expression of opsin-encoding genes in a (spatially targeted) subpopulation of neurons. Recently, systems that allow light-activated (exogenous) gene expression have been created using functional dimerization of phytochrome proteins [101] and proteins having light oxygen voltage (LOV) sensing [102] or Blue-Light-Utilizing flavin adenine dinucleotide

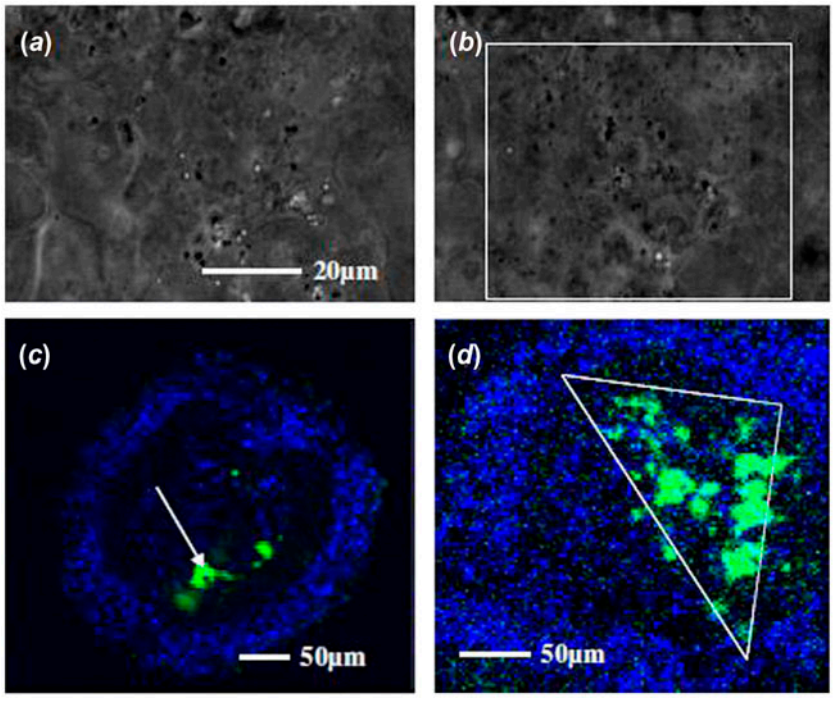

Figure 10. Optoporation of ChR2 genes into targeted area of retina. (*a*) bright field image of a retina explant; (*b*) array of dark spots created after patterned irradiation with ultrafast laser microbeam; (*c*) highly localized laser ChR2-YFP transfection of retina explant, immunostained for YFP and co-stained nucleus with DAPI; (*d*) Triangular region transfected with ChR2-YFP by patterned NIR fs laser microbeam [78]. (The color version of this figure is included in the online version of the journal.)

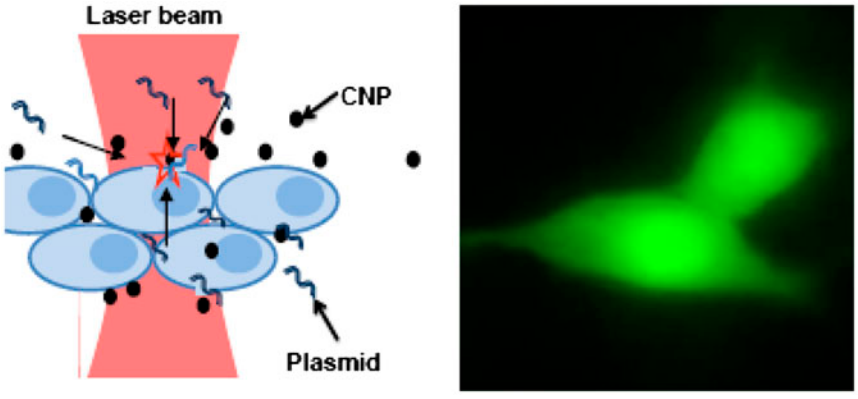

Figure 11. PTD of ChR2 genes into targeted cells. Left: Principle of carbon nanoparticles-mediated photothermal delivery using CW laser beam. Right: YFP-fluorescence confirming photothermal delivery (PTD) of ChR2-YFP encoding plasmids into cells using CW NIR laser beam. (The color version of this figure is included in the online version of the journal.)

(FAD) (BLUF) domains [103,104] upon light activation. Upon blue light illumination, the LOV/BLUF proteins undergo a conformational change to activate the attached effector domain. Similarly, phytochromes are responsive to red and far-red light absorption to manipulate target gene expression. The ability to control protein function with the spatial and temporal resolution of a beam of light has opened up new avenues to study cell migration [105], cell morphology [106], and more.

6. Non-linear optogenetic stimulation

Conventional optogenetic activation [49–55] requires light wavelengths in visible spectrum (e.g. 460 nm for ChR2), where significant absorption and scattering of the stimulating light occurs. However, the use of visible (single photon) light has significant limitations in stimulating localized area of brain as: (1) 90% of the incident power is lost (within 1 mm for blue light) due to scattering and absorption within the neural tissue; therefore,

necessitating placement of the optical fiber near the targeted region, thus damaging the dorsal regions, (2) extended periods of illumination can cause damage to the neurons, and (3) it relies on non-localized (out-of-target) stimulation. To overcome these limitations, Mohanty et al. [107] reported NIR two-photon optogenetic activation of HEK cells and brain slices. Since this time significant progress has been made using two-photon optogenetic stimulation beam for probing neural circuitry in cultured neuronal cells and cortical slices [108]. Other advances demonstrate that optogenetically sensitized neurons can be activated by spatially sculpting and/or temporal focusing of the two-photon beam [109]. It is important to note here that different scanning modes (spiral, raster) have been applied for the excitation of ChR2-expressing cells to optimize the efficiency of excitation [110]. Because of low scattering (and absorption) coefficients of brain tissue in the NIR spectrum, two-photon optogenetic activation using NIR laser beam can provide deep penetration. High spatial precision is achieved by virtue of non-linear nature of ultrafast light interaction with ChR2 (Figure 12(*a*)). There have been recent advancements in two-photon optogenetic stimulation technology by spatial sculpting [111] and/or temporal focusing [112] of the laser microbeam (focused by microscopic objective). Unlike single-photon light, two-photon NIR stimulation is spatially localized, less invasive in terms of both surgery-related injury and optically induced damage to the neurons. Therefore, two-photon optogenetics permits probing the neuronal circuitry in central nervous system and also allows subcellular stimulation. Figure 12(*b*) shows increases in calcium fluorescence subsequent to patterned stimulation of cells caused by raster-scanning NIR laser beam.

Two-photon optogenetic activation has also been possible using weakly focused light and even fiber-optic beams (Figure 13) [113]. Either single mode or multimode fiber can be used (Figure 13(*a*)). It may be noted that the two-photon cross section of ChR2 has been estimated [114] to be very high (~250 GM), higher than even several fluorophores. While cleaved fiber-optic beam can also lead to two-photon fluorescence excitation (Figure 13(*b*)) and optogenetic activation (Figure 13(*c*)), lensed fiber-optic beam (Figure 13(*a*)) can provide focal stimulation in addition to deeper penetration. Figure 13(*c*) shows representative inward current responses due to fiber-optic ultrafast NIR (850 nm) stimulation of a HEK-ChR2 cell at different average power densities. The dependence of two-photon (at 850 nm, 100 ms pulses)-induced inward current as a function of incident average power densities (near the cell membrane) is shown in Figure 13(*d*). In contrast to non-linear response of inward current, the induced current in cells is found to be linearly dependent on the incident average two-photon laser power density. Unlike two-photon fluorescence excitation, two-photon optogenetic stimulation of ChR2-sensitized cells is not a single-step process. This is due to the fact that in case of optogenetic activation, inward current is associated with conformational change of the molecule rather than a simple two-level transition as in case of dye molecule. Therefore, along with intensity, other parameters such as the kinetics of the opening of

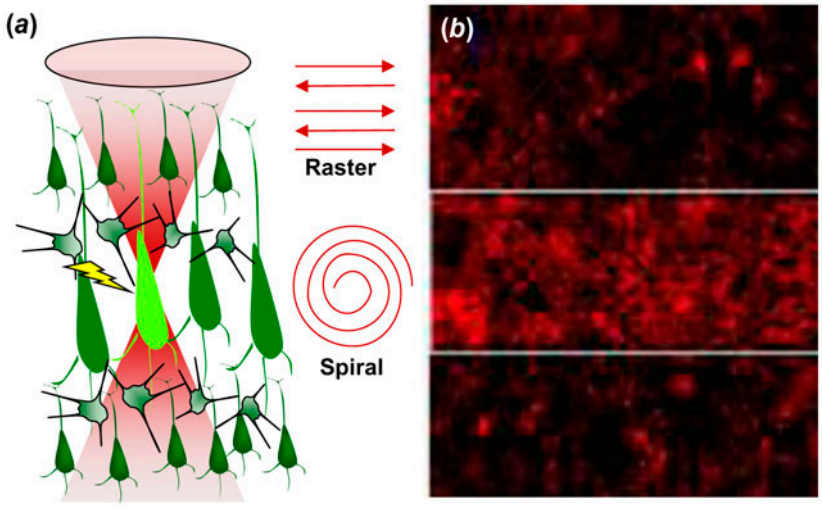

Figure 12. Focused two-photon NIR beam increases target-specific stimulation (↘) compared to single photon. (*a*) Schematics of localized stimulation of target neuron by non-linear interaction of ultrafast NIR laser microbeam. (*b*) Activation of spatially targeted HEK-ChR2 cells (by scanning two-photon NIR beam) visualized by rise in intracellular calcium. (The color version of this figure is included in the online version of the journal.)

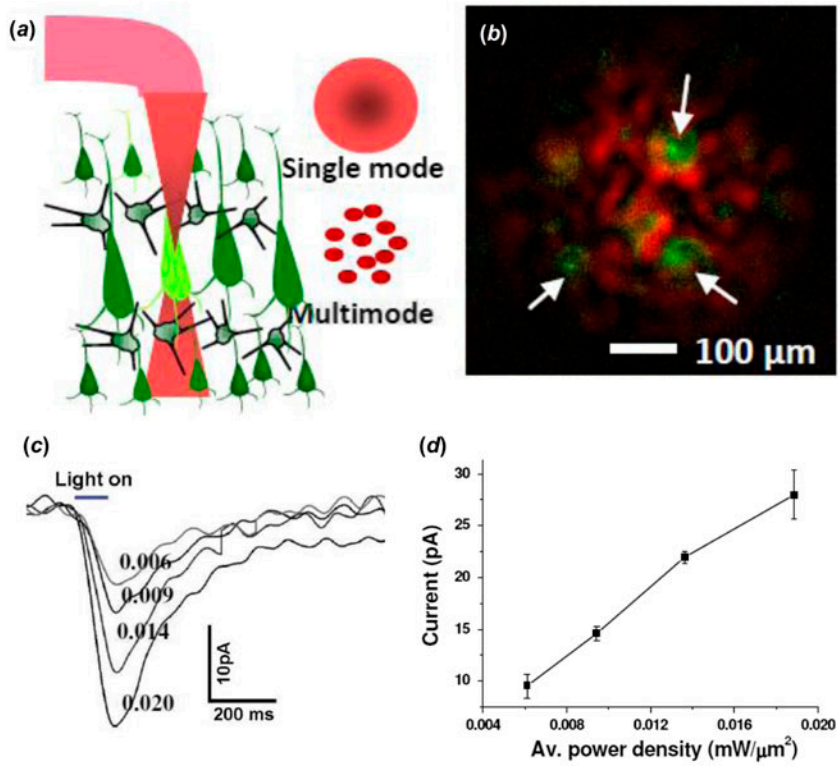

Figure 13. Fiber-optic NIR beam for two-photon optogenetic stimulation. (*a*) Schematic of fiber-optic two-photon optogenetic activation. (*b*) Composite image of two-photon fluorescence from polystyrene particles (green) and excitation intensity pattern (red). (*c*) Inward current responses due to fiber-optic two-photon beam (850 nm) at different average power densities. (*d*) Dependence of inward current as a function of power densities (100 ms pulses) [113]. (The color version of this figure is included in the online version of the journal.)

the ChR2-channel and two-photon absorption of ATR [115,116] may modulate the nature of intensity-dependent current variations.

The peak of the two-photon activation spectrum of ChR2 has been observed to be around 850 nm, which is significantly blue-shifted from the double of single-photon activation peak at 460 nm. Recently, *in vivo* fiber-optic two-photon optogenetic stimulation of dopaminergic neurons at depths of 3 mm has been demonstrated, thus allowing cell-specific, non-invasive, and deep brain stimulation [117]. Based on the low two-photon activation threshold, it may be possible to use nanosecond or microsecond compact NIR sources for this purpose. This will be of significant advantage for deep brain optogenetic stimulation and animal studies as compared to bulky and expensive fs laser systems. Further, use of microlens or axicon [118] on fiber tip should allow focus control of the fiber-optic two-photon beam. By tuning the wavelength of the two-photon light source for other opsins such as NpHR, the fiber-optic method can be useful for combinatorial modulation (both excitation as well as inhibition) of the neural activity. The fiber-optic two-photon optogenetic technology will allow in-depth probing of neural circuitry *in vivo* since this technology permits minimally invasive and more precise anatomical delivery of stimulation (Figure 14). Further, due to compactness and flexibility of the fiber, it would allow study of neuromodulation in freely behaving animals. Using the technology already developed for non-linear endoscopy [119], both two-photon stimulation and optical imaging of neural activity can be achieved *in vivo*.

7. Optical recording of cellular activity

Contemporary *in vitro*, and (especially) *in vivo* neuroscience research studies require the simultaneous mapping/measurement of large populations (or networks) of interconnected cells. This becomes increasingly invasive, and often logistically impossible with traditional electrode-based recording methods. Despite the sensitivity, reproducibility, and temporal resolution of patch clamp recordings, there have been significant efforts to find alternative methods for measuring voltage differences and action potentials in neurons. Electrodes have limited spatial resolution and since electrode methodologies rely on mechanical stability, it is cumbersome to use. Further, electrophysiological detection from every

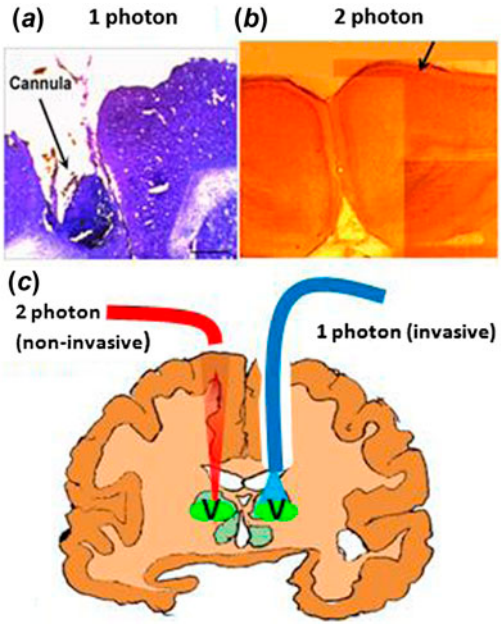

Figure 14. Non-invasiveness of two-photon optogenetic stimulation. (*a*) Brain tissue damage by optical fiber delivering one-photon beam. (*b*) Non-invasive two-photon beam. (*c*) Schematic comparison of one-photon vs. two-photon optogenetic stimulation (V = ventral targeted region of the brain). (The color version of this figure is included in the online version of the journal.)

single opsin-expressing cell would require electrodes implanted inside tissue in every cell of the specific class and in that case, even *in vitro* detection from depth of a tissue slice is not feasible. In contrast, optical methods are being developed that allows detection large number of cells simultaneously. With the advent of voltage sensitive dyes (VSDs), it was demonstrated that membrane potential information could be detected optically with increased spatial information, while eliminating cellular damage.

VSDs are an ever-expanding collection of organic molecules and proteins whose optical properties change dynamically in the presence of changing electric potential (voltage) or ion transport across the cell membrane. These dyes indicate the variation in electrical potential based on the variation of their absorbance, fluorescence intensity, fluorescence spectrum, or birefringence from 'resting' values. These molecules usually have a hydrophobic portion that sticks to the membrane and a charged chromophore that prevents crossing to the cell interior. These dyes have a high absorption coefficient and usually high quantum efficiency for use with neuronal cells. Classical VSDs are typically split into two groups (although the distinction is often vague) based on their response time, and are unimaginatively referred to as slow and fast dyes. Slow dyes give rise to relatively large variations in fluorescence intensity (0.1–1% per millivolt of depolarization) which can typically be monitored with conventional spectrometers/detectors. However, their response time (milliseconds to seconds) makes them unsuitable for monitoring rapid neuronal activity. Slow dyes are most useful in establishing baseline ('resting') potentials for large cell populations. Fast dyes have a response time on the order of microseconds. For example, neurons stained with the mixture of dyes (merocyanine-540 and rhodamine-123) have a response time of less than 10 μs. Although the measurable variations in fluorescence intensity are smaller than in the case of slow dyes, improved fluorescence yield and more sophisticated detection equipment allow for the detection of action potentials without averaging. Furthermore, the measured intensities are generally linear with changes in membrane potential. The main advantages of using VSDs over classical patch clamp techniques are that the optical method is technically less invasive and that it can be applied to large populations. By eliminating inherent damage incurred during electrode-based techniques, electric potential measurements can be taken of structures traditionally too fragile to survive patch clamp, such as axons and growth cones. VSDs have been used to whole organs, and to monitor large populations of cells simultaneously. Additionally, VSD imaging can be readily combined with other imaging techniques, such as confocal microscopy, ion concentration imaging, or selective optical stimulation. The combination of wavelengths of different laser beams has permitted simultaneous identification of opsin-reporter expression and monitoring of the optogenetic activation process in multiple cells. Subsequent to optogenetic activation of ChR2-expressing cells, change in intracellular Ca^{2+} levels are monitored using a Ca^{2+}-sensitive dye (calcium orange) that was excited with a 543 nm He–Ne laser beam. Since Ca-orange has excitation wavelength ~550 nm, it does not overlap with ChR2-activation band. Further, its fluorescence (>590 nm) is far from YFP fluorescence making it easier to distinguish calcium signal from YFP fluorescence. Figure 15(*a*) shows ChR2-YFP expressing (green) HEK cells stained with calcium orange (red). The increase in Ca-orange fluorescence from a localized region on membrane of a HEK-ChR2 cell (Figure 15(*a*)) during two-photon optogenetic stimulation is shown in Figure 15(*b*), which attains basal fluorescence after switching off the stimulation.

The most important disadvantage in using classical VSDs is that, while they are obviously less mechanically invasive, there are still both pharmacological and phototoxic side effects to consider. In the case of neurons, organic molecules are susceptible to non-specific binding, and may bind directly to ion channels or other intracellular components, modifying their function (conductance, neurotransmitter functionality). Furthermore, the cell membrane may become damaged during prolonged or repeated illumination, as certain organic dye

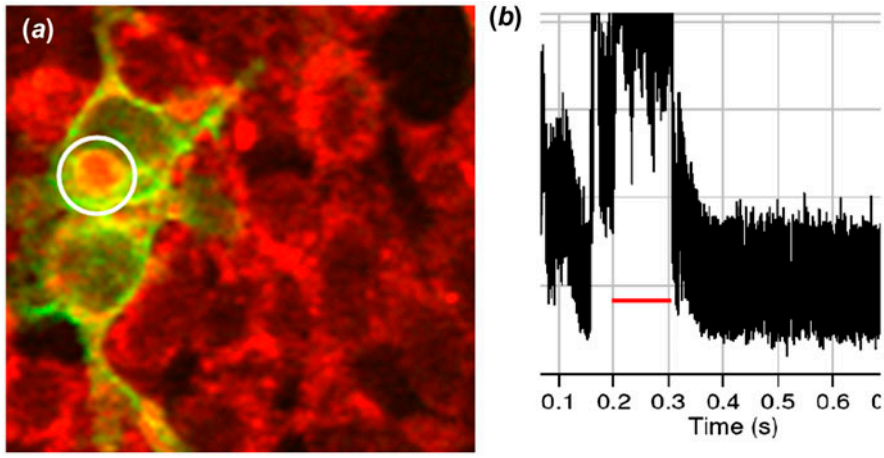

Figure 15. Calcium imaging of optogenetic activation of cells. (*a*) ChR2-YFP expressing (green) cells stained with ca orange (red). (*b*) Kinetics of Ca orange fluorescence from the stimulated region of the ChR2-expressing cell (marked by circle in *a*). (The color version of this figure is included in the online version of the journal.)

molecules, while in their excited state, are more reactive with oxygen molecules, creating singlet oxygen radicals. These highly reactive radicals can lead to oxidation of membrane bound proteins, effectively damaging the cell. The researcher is thus left with a serious conundrum. Increased dye concentration and increased illumination intensity will lead to high fluorescence intensity, but high dye concentrations and illumination intensities modify cell function, bleach the dye, and/or increase the potential of cell damage. The optimization of these parameters is therefore necessary. Additionally, it is often required that dyes be calibrated with traditional electrode-based recording methods before or in parallel with optical recordings, leading to experimental redundancy.

VSDs, which bind to the surface of cellular membranes, have several practical flaws. However, the flaws discussed up to this point are more practical problems than actual limitations. New dyes may have higher efficiencies and lower toxicities, but there are some flaws that are actual limiting factors of classical VSDs. In the study of neural circuitry, it is often necessary that there be several types of neurons present in a single dish or organ. Assuming a standard dye and application technique, the dye will diffuse over time and bind to all cell membranes in a sample. This will create two problems: a high background, and a lack of cell (type) selectivity. These problems are currently being addressed with the development of GEVI [120]. GEVI are protein sensors, which are selectively expressed by cell-specific promoters. In this way, subpopulations of neurons within a larger network can be specifically monitored. Furthermore, these protein sensors may even be expressed in known, specific portions or components of cell subpopulations (i.e. dendrites) so that electrical potentials can be monitored within structures which cannot be optically resolved in a conventional manner, leading to new possibilities in the realm of neural activity imaging. To characterize neural activities *in vitro* or *in vivo* stimulated optogenetically, there is a need for deployment of functional optical imaging method having high spatial and temporal resolution. Since GEVIs or genetically encoded calcium indicator (GECI) can be genetically targeted [121], it provides the cell specificity and changes in GEVI or GECI fluorescence can be monitored in mammalian cells and organisms [122]. GCaMP is a GECI that provide less cytotoxicity and stable (less photobleaching) fluorescence over the observation period and has undergone progressive modifications (e.g. GCaMP3 [123]) for enhanced fluorescence signal. Use of GECI-based optical recording method has overcome the disadvantages associated with mechanical perturbations during electrical recordings and cytotoxicity related to chemical agents such as dyes. Such functional (calcium, voltage sensitive probe) imaging can be achieved using conventional/plane illumination microscopy depending on the sample size of interest. With optical detection of neural activities, the whole process of identification, activation, and detection can be made non-invasive added with the advantages of high throughput and least requirement of mechanical stability and contamination.

An ideal optical method for monitoring cell activity should be less invasive both mechanically (implying no electrodes) and chemically (i.e. no added markers or dyes for fluorescence imaging). While use of GEVI will provide less cytotoxicity, photobleaching of the fluorescence may hinder long-term recording of neural activity. Using phase information obtained from an optical interferometric technique, it is possible to non-invasively measure changes in optical path length of the neurons

(due to either nanoscale volumetric changes or changes in refractive index) during stimulation regimes without requiring addition of dyes or genetic voltage/ion indicators. Recently, use of Phase-Sensitive Optical Coherence Tomography (PSFD-OCT) has demonstrated [124] label-free imaging of cellular activity during optogenetic stimulation. PSFD-OCT is a novel technique based on the principles of low-coherence interferometry that can detect displacements of the order of tens of picometers [125–129] by analyzing the phase changes in the measured spectral interferograms. In FD-OCT, the interference signal is detected by a linear array of CCD and then Fourier transformed (FT) to obtain the structural image (amplitude of the Fourier transformed signal). In PSFD-OCT, the phase of the FT signal is analyzed to detect nanomotion. In PSFD-OCT, the reference mirror is stationary and the interference signal between the reflected intensities from the reference mirror and the cell microstructures is detected with a spectrometer as a function of wavelength. The detected signal (as a function of wavelength) is then Fourier transformed to obtain intensity profile as a function of depth. FD-OCT scans the whole depth of the sample without any mechanical scanning, which leads to higher phase stability. However, since PSFD-OCT-based phase measurement is a point scanning method, quantitative phase microscopy using wide-field methods such as digital holographic microscopy can be developed for label-free imaging of activity of the optogenetically activated cells.

8. Conclusions and future outlook

The laser-assisted delivery/expression of genes in spatially targeted regions will help in controlled functionalization of neurons by opsin expression. In addition, the electrical activity (activation/silencing) of specific neurons in a brain region can be controlled by optical stimulation; thus, encoding activities in specific neurons and modulating overall behavior of an organism. The two-photon optogenetic method is paving the way for precise *in vivo* probing of neural circuitry in a minimally invasive manner. Besides obtaining structural information, optical imaging methods holds promise to non-invasively record the neural activity. All-optical control of neural circuitry (Figure 16) using NIR laser beam includes (i) functionalization of the targeted neurons by NIR laser transfection; (ii) modulation of the activity by optical and optogenetic stimulation; and (iii) deciphering the neural code in a label-free manner. The all-optical approach for control and monitoring of neural circuitry will allow better understanding of signal processing by single neuron and its contribution to the functioning of the complex neuronal circuitry.

The challenges in development of optogenetic stimulation/inhibition include: (i) increasing the ion selectivity, light sensitivity, and kinetics of the opsins; (ii) better control on delivery/expression of opsin constructs in the targeted cells as well as trafficking to cell membrane; (iii) narrowing spectral response for allowing use of multiple opsins in multiple cell types simultaneously;

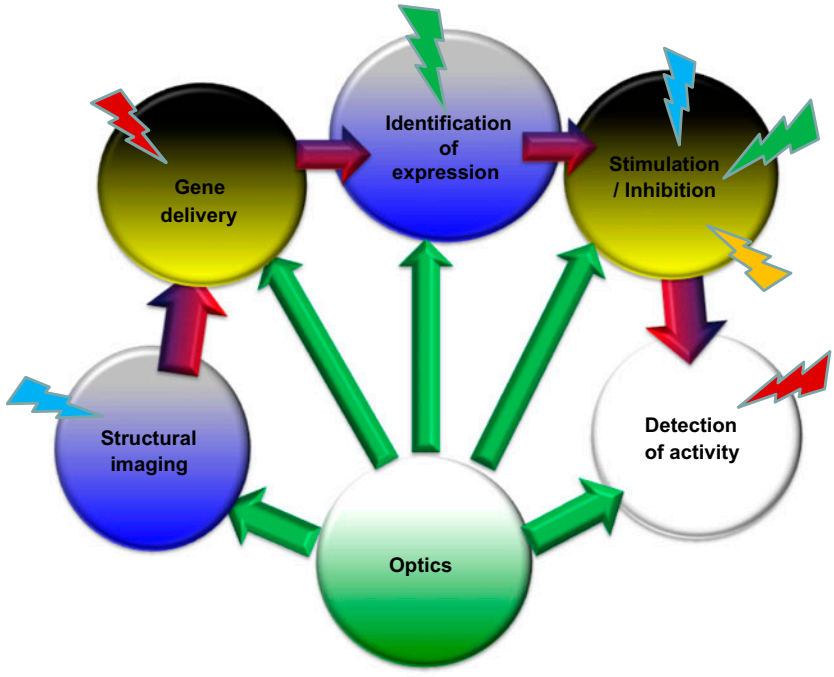

Figure 16. All-optical control of optogenetics and associated methods for imaging, gene delivery, expression analysis, activation of opsin along with detection of neural activity. (The color version of this figure is included in the online version of the journal.)

(iv) use of compact NIR light source and/or red-shifted activation spectrum for deeper and/or localized stimulation/inhibition; (v) use of diffractive and/or adaptive optics for generation of spatially and/or phase-modulated beams in order to allow more precise stimulation; and (vi) wide-field label-free optical imaging of neural activities with high temporal resolution, at larger depths.

Acknowledgments

The primary author (SM) is indebted to the collaborators, co-workers and students involved with his group in optogenetic research. Special thanks to Dr Young-tae Kim and Dr Bryan Black (UTA) for help in preparation of some portion of the text and figures. SM would also like to thank the support from Office of President and Provost, The University of Texas at Arlington and the National Science Foundation (1148541) and National Institute of Health (NS084311). Apologies to all the authors whose excellent work could not be included due to limitation on space.

Funding

This work was supported by the University of Texas at Arlington and the National Science Foundation [grant number 1148541]; National Institute of Health [grant number NS084311].

References

[1] Oesterhelt, D. *Curr. Opin. Struct. Biol.* **1998,** *8,* 489–500.
[2] Haupts, U.; Tittor, J.; Oesterhelt, D. *Annu. Rev. Biophys. Biomol. Struct.* **1999,** *28,* 367–399.
[3] Kolbe, M.; Besir, H.; Essen, L.O.; Oesterhelt, D. *Science* **2000,** *288,* 1390–1396.
[4] Okuno, D.; Asaumi, M.; Muneyuki, E. *Biochemistry* **1999,** *38,* 5422–5429.
[5] Zemelman, B.V.; Lee, G.A.; Ng, M.; Miesenböck, G. *Neuron* **2002,** *33,* 15–22.
[6] Nagel, G.; Szellas, T.; Huhn, W.; Kateriya, S.; Adeishvili, N.; Berthold, P.; Ollig, D.; Hegemann, P.; Bamberg, E. *Proc. Natl. Acad. Sci. USA.* **2003,** *100,* 13940–13945.
[7] Boyden, E.S.; Zhang, F.; Bamberg, E.; Nagel, G.; Deisseroth, K. *Nat. Neurosci.* **2005,** *8,* 1263–1268.
[8] Nagel, G.; Brauner, M.; Liewald, J.F.; Adeishvili, N.; Bamberg, E.; Gottschalk, A. *Curr. Biol.* **2005,** *15,* 2279–2284.
[9] Miller, G. *Science* **2006,** *314,* 1674–1676.
[10] Yizhar, O.; Fenno, L.E.; Davidson, T.J.; Mogri, M.; Deisseroth, K. *Neuron* **2011,** *71,* 9–34.
[11] Boyden, E.S. *F1000 Biol. Rep.* **2011,** 3, 11.
[12] Fenno, L.; Yizhar, O.; Deisseroth, K. *Annu. Rev. Neurosci.* **2011,** *34,* 389–412.
[13] Adamantidis, A.R.; Zhang, F.; de Lecea, L.; Deisseroth, K. *Cold Spring Harbor Protoc.* **2014,** *2014,* 815–822.
[14] Gradinaru, V.; Zhang, F.; Ramakrishnan, C.; Mattis, J.; Prakash, R.; Diester, I.; Goshen, I.; Thompson, K.R.; Deisseroth, K. *Cell* **2010,** *141,* 154–165.
[15] Mei, Y.; Zhang, F. *Biol. Psychiatry* **2012,** *71,* 1033–1038.
[16] Li, X.; Gutierrez, D.V.; Hanson, M.G.; Han, J.; Mark, M.D.; Chiel, H.; Hegemann, P.; Landmesser, L.T.; Herlitze, S. *Proc. Natl. Acad. Sci. USA.* **2005,** *102,* 17816–17821.
[17] Ishizuka, T.; Kakuda, M.; Araki, R.; Yawo, H. *Neurosci. Res.* **2006,** *54,* 85–94.
[18] Han, X.; Boyden, E.S. *PLoS One* **2007,** *2,* e299.
[19] Zhang, F.; Wang, L.P.; Brauner, M.; Liewald, J.F.; Kay, K.; Watzke, N.; Wood, P.G.; Bamberg, E.; Nagel, G.; Gottschalk, A.; Deisseroth, K. *Nature* **2007,** *446,* 633–639.
[20] Kato, H.E.; Zhang, F.; Yizhar, O.; Ramakrishnan, C.; Nishizawa, T.; Hirata, K.; Ito, J.; Aita, Y.; Tsukazaki, T.; Hayashi, S.; Hegemann, P.; Maturana, A.D.; Ishitani, R.; Deisseroth, K.; Nureki, O. *Nature* **2012,** *482,* 369–374.
[21] Lin, J.Y.; Knutsen, P.M.; Muller, A.; Kleinfeld, D.; Tsien, R.Y. *Nat. Neurosci.* **2013,** *16,* 1499–1508.
[22] Kleinlogel, S.; Feldbauer, K.; Dempski, R.E.; Fotis, H.; Wood, P.G.; Bamann, C.; Bamberg, E. *Nat. Neurosci.* **2011,** *14,* 513–518.
[23] Chow, B.Y.; Han, X.; Dobry, A.S.; Qian, X.; Chuong, A.S.; Li, M.; Henninger, M.A.; Belfort, G.M.; Lin, Y.; Monahan, P.E.; Boyden, E.S. *Nature* **2010,** *463,* 98–102.
[24] Davidson, B.L.; Breakefield, X.O. *Nat. Rev. Neurosci.* **2003,** *4,* 353–364.
[25] Cetin, A.; Komai, S.; Eliava, M.; Seeburg, P.H.; Osten, P. *Nat. Protoc.* **2006,** *1,* 3166–3173.
[26] Aravanis, A.M.; Wang, L.P.; Zhang, F.; Meltzer, L.A.; Mogri, M.Z.; Schneider, M.B.; Deisseroth, K. *J. Neural Eng.* **2007,** *4,* S143–S156.
[27] Chhatwal, J.P.; Hammack, S.E.; Jasnow, A.M.; Rainnie, D.G.; Ressler, K.J. *Gene Ther.* **2007,** *14,* 575–583.
[28] Taymans, J.M.; Vandenberghe, L.H.; Haute, C.V.; Thiry, I.; Deroose, C.M.; Mortelmans, L.; Wilson, J.M.; Debyser, Z.; Baekelandt, V. *Hum. Gene Ther.* **2007,** *18,* 195–206.
[29] Wickersham, I.R.; Finke, S.; Conzelmann, K.K.; Callaway, E.M. *Nat. Methods* **2007,** *4,* 47–49.
[30] Grossman, N.; Poher, V.; Grubb, M.S.; Kennedy, G.T.; Nikolic, K.; McGovern, B.; Palmini, R.B.; Gong, Z.; Drakakis, E.M.; Neil, M.A. *J. Neural Eng.* **2010,** *7,* 016004.
[31] Tokuda, T.; Kimura, H.; Miyatani, T.; Maezawa, Y.; Kobayashi, T.; Noda, T.; Sasagawa, K.; Ohta, J. *Electron. Lett.* **2012,** *48,* 312–314.
[32] Wang, L.; Jacques, S.L.; Zheng, L. *Comput. Methods Programs Biomed.* **1995,** *47,* 131–146.
[33] Boas, D.; Culver, J.; Stott, J.; Dunn, A. *Opt. Express* **2002,** *10,* 159–170.
[34] Wang, L.H.; Jacques, S.L.; Zheng, L.Q. *Comput. Methods Programs Biomed.* **1995,** *47,* 131–146.
[35] Wang, L.; Jacques, S.L.; Zheng, L. *Comput. Methods Programs Biomed.* **1997,** *54,* 141–150.
[36] Johansson, J.D. *J. Biomed. Opt.* **2010,** *15,* 057005.
[37] Yaroslavsky, A.N.; Schulze, P.C.; Yaroslavsky, I.V.; Schober, R.; Ulrich, F.; Schwarzmaier, H.J. *Phys. Med. Biol.* **2002,** *47,* 2059–2073.
[38] Cheong, W.F.; Prahl, S.A.; Welch, A.J. *IEEE J. Quantum Electron.* **1990,** *26,* 2166–2185.
[39] Cao, H.; Gu, L.; Mohanty, S.K.; Chiao, J.C. *IEEE Trans. Biomed. Eng.* **2013,** *60,* 225–229.
[40] Kim, T.I.; McCall, J.G.; Jung, Y.H.; Huang, X.; Siuda, E.R.; Li, Y.; Song, J.; Song, Y.M.; Pao, H.A.; Kim, R.H.; Lu, C.; Lee, S.D.; Song, I.; Shin, G.; Al-Hasani, R.; Kim, S.; Tan, M.P.; Huang, Y.; Omenetto, F.G.; Rogers, J.A.; Bruchas, M.R. *Science* **2013,** *340,* 211–216.
[41] Zhang, F.; Wang, L.-P.; Boyden, E.S.; Deisseroth, K. *Nat. Methods* **2006,** *3,* 785–792.

[42] Nagel, G.; Szellas, T.; Huhn, W.; Kateriya, S.; Adeishvili, N.; Berthold, P.; Ollig, D.; Hegemann, P.; Bamberg, E. *Proc. Natl. Acad. Sci. USA.* **2003,** *100,* 13940–13945.
[43] Pastrana, E. *Nat. Methods* **2011,** *8,* 24–25.
[44] Fenno, L.; Yizhar, O.; Deisseroth, K. *Annu. Rev. Neurosci.* **2011,** *34,* 389–412.
[45] Janovjak, H.; Szobota, S.; Wyart, C.; Trauner, D.; Isacoff, E.Y. *Nat. Neurosci.* **2010,** *13,* 1027–1032.
[46] Boyden, E.S.; Zhang, F.; Bamberg, E.; Nagel, G.; Deisseroth, K. *Nat. Neurosci.* **2005,** *8,* 1263–1268.
[47] Nagel, G.; Brauner, M.; Liewald, J.F.; Adeishvili, N.; Bamberg, E.; Gottschalk, A. *Curr. Biol.* **2005,** *15,* 2279–2284.
[48] Llewellyn, M.E.; Thompson, K.R.; Deisseroth, K.; Delp, S.L. *Nat. Med.* **2010,** *16,* 1161–1165.
[49] Lagali, P.S.; Balya, D.; Awatramani, G.B.; Münch, T.A.; Kim, D.S.; Busskamp, V.; Cepko, C.L.; Roska, B. *Nat. Neurosci.* **2008,** *11,* 667–675.
[50] Ivanova, E.; Roberts, R.; Bissig, D.; Pan, Z.-H.; Berkowitz, B.A. *Mol. Vision* **2010,** *16,* 1059–1067.
[51] Tomita, H.; Sugano, E.; Fukazawa, Y.; Isago, H.; Sugiyama, Y.; Hiroi, T.; Ishizuka, T.; Mushiake, H.; Kato, M.; Hirabayashi, M.; Shigemoto, R.; Yawo, H.; Tamai, M. *PLoS One* **2009,** *4,* e7679.
[52] Lobo, M.K.; Covington, H.E.; Chaudhury, D.; Friedman, A.K.; Sun, H.; Damez-Werno, D.; Dietz, D.M.; Zaman, S.; Koo, J.W.; Kennedy, P.J.; Mouzon, E.; Mogri, M.; Neve, R.L.; Deisseroth, K.; Han, M.; Nestler, E.J. *Science* **2010,** *330,* 385–390.
[53] Stuber, G.D. *Neuropsychopharmacology* **2010,** *35,* 341–342.
[54] Johansen, J.P.; Hamanaka, H.; Monfils, M.H.; Behnia, R.; Deisseroth, K.; Blair, H.T.; LeDoux, J.E. *Proc. Natl. Acad. Sci. USA.* **2010,** *107,* 12692–12697.
[55] Tønnesen, J.; Parish, C.L.; Sørensen, A.T.; Andersson, A.; Lundberg, C.; Deisseroth, K.; Arenas, E.; Lindvall, O.; Kokaia, M. *PLoS One* **2011,** *6,* e17560.
[56] Hartong, D.T.; Berson, E.L.; Dryja, T.P. *The Lancet* **2006,** *368,* 1795–1809.
[57] Sugawara, T.; Hagiwara, A.; Hiramatsu, A.; Ogata, K.; Mitamura, Y.; Yamamoto, S. *Eye* **2010,** *24,* 535–539.
[58] Daiger, S.P.; Bowne, S.J.; Sullivan, L.S. *Arch. Ophthalmol.* **2007,** *125,* 151–158.
[59] Mezer, E.; Babul-Hirji, R.; Wise, R.; Chipman, M.; DaSilva, L.; Rowell, M.; Thackray, R.; Shuman, C.T.; Levin, A.V. *Ophthalmic Genet.* **2007,** *28,* 9–15.
[60] Baumgartner, W.A. *Med. Hypotheses* **2000,** *54,* 814–824.
[61] Hamel, C. *Orphanet J. Rare Dis.* **2006,** *1,* 40.
[62] Horsager, A.; Greenwald, S.H.; Weiland, J.D.; Humayun, M.S.; Greenberg, R.J.; McMahon, M.J.; Boynton, G.M.; Fine, I. *Invest. Ophthalmol. Visual Sci.* **2009,** *50,* 1483–1491.
[63] de Balthasar, C.; Patel, S.; Roy, A.; Freda, R.; Greenwald, S.; Horsager, A.; Mahadevappa, M.; Yanai, D.; McMahon, M.J.; Humayun, M.S.; Greenberg, R.J.; Weiland, J.D.; Fine, I. *Invest. Ophthalmol. Visual Sci.* **2008,** *49,* 2303–2314.
[64] Zrenner, E.; Bartz-Schmidt, K.U.; Benav, H.; Besch, D.; Bruckmann, A.; Gabel, V.P.; Gekeler, F.; Greppmaier, U.; Harscher, A.; Kibbel, S.; Koch, J.; Kusnyerik, A.; Peters, T.; Stingl, K.; Sachs, H.; Stett, A.; Szurman, P.; Wilhelm, B.; Wilke, R. *Proc. Biol Sci.* **2011,** *278,* 1489–1497.
[65] Zrenner, E. *Science* **2002,** *295,* 1022–1025.
[66] Eckmiller, R. *Ophthalmic Res.* **1997,** *29,* 281–289.
[67] Chow, A.Y.; Pardue, M.T.; Perlman, J.I.; Ball, S.L.; Chow, V.Y.; Hetling, J.R.; Peyman, G.A.; Liang, C.; Stubbs, J.; Evan, B.; Peachey, N.S. *J. Rehabil. Res. Dev.* **2002,** *39,* 313–321.
[68] Thyagarajan, S.; van Wyk, M.; Lehmann, K.; Lowel, S.; Feng, G.; Wassle, H. *J. Neurosci.* **2010,** *30,* 8745–8758.
[69] Bi, A.; Cui, J.; Ma, Y.P.; Olshevskaya, E.; Pu, M.; Dizhoor, A.M.; Pan, Z.H. *Neuron* **2006,** *50,* 23–33.
[70] Zhang, Y.; Ivanova, E.; Bi, A.; Pan, Z.-H. *J. Neurosci.* **2009,** *29,* 9186–9196.
[71] Tomita, H.; Sugano, E.; Isago, H.; Hiroi, T.; Wang, Z.; Ohta, E.; Tamai, M. *Exp. Eye Res.* **2010,** *90,* 429–436.
[72] Busskamp, V.; Duebel, J.; Balya, D.; Fradot, M.; Viney, T.J.; Siegert, S.; Groner, A.C.; Cabuy, E.; Forster, V.; Seeliger, M.; Biel, M.; Humphries, P.; Paques, M.; Mohand-said, S.; Trono, D.; Deisseroth, K.; Sahel, J.A.; Picaud, S.; Roska, B. *Science* **2010,** *329,* 413–417.
[73] Shivalingaiah, S.; Gu, L.; Mohanty, S.K. *Proc. SPIE* **2011,** *7885,* 78851Y.
[74] Cao, H.; Gu, L.; Mohanty, S.K.; Chiao, J.C. *IEEE Trans. Biomed. Eng.* **2013,** *60,* 225–229.
[75] Han, X.; Qian, X.; Bernstein, J.G.; Zhou, H.H.; Franzesi, G.T.; Stern, P.; Bronson, R.T.; Graybiel, A.M.; Desimone, R.; Boyden, E.S. *Neuron* **2009,** *62,* 191–198.
[76] Tao, W.; Wilkinson, J.; Stanbridge, E.J.; Berns, M.W. *Proc. Natl. Acad. Sci. USA.* **1987,** *84,* 4180–4184.
[77] Tirlapur, U.K.; König, K. *Nature* **2002,** *418,* 290–291.
[78] Gu, L.; Mohanty, S.K. *J. Biomed. Opt.* **2011,** *16,* 128003–128006.
[79] Stevenson, D.; Agate, B.; Tsampoula, X.; Fischer, P.; Brown, C.T.A.; Sibbett, W.; Riches, A.; Gunn-Moore, F.; Dholakia, K. *Opt. Express* **2006,** *14,* 7125–7133.
[80] Soman, P.; Zhang, W.D.; Umeda, A.; Zhang, Z.J.; Chen, S.C. *J. Biomed. Nanotechnol.* **2011,** *7,* 334–341.
[81] Stracke, F.; Rieman, I.; König, K. *J. Photochem. Photobiol. B* **2005,** *81,* 136–142.
[82] Barrett, L.E.; Sul, J.Y.; Takano, H.; Van Bockstaele, E.J.; Haydon, P.G.; Eberwine, J.H. *Nat. Methods* **2006,** *3,* 455–460.
[83] Stevenson, D.; Agate, B.; Tsampoula, X.; Fischer, P.; Brown, C.T.A.; Sibbett, W.; Riches, A.; Gunn-Moore, F.; Dholakia, K. *Opt. Express* **2006,** *14,* 7125–7133.
[84] Peng, C.; Palazzo, R.E.; Wilke, I. *Phys. Rev. E* **2007,** *75,* 041903.
[85] Kohli, V.; Elezzabi, A.Y. *BMC Biotechnol.* **2008,** *8,* 7.
[86] Tsampoula, X.; Garcés-Chávez, V.; Comrie, M.; Stevenson, D.J.; Agate, B.; Brown, C.T.A.; Gunn-Moore, F.; Dholakia, K. *Appl. Phys. Lett.* **2007,** 91*,* 053902.
[87] Tsampoula, X.; Taguchi, K.; Cižmár, T.; Garces-Chavez, V.; Ma, N.; Mohanty, S.; Mohanty, K.; Gunn-Moore, F.; Dholakia, K. *Opt. Express* **2008,** *16,* 17007–17013.
[88] Brown, C.T.A.; Stevenson, D.J.; Tsampoula, X.; McDougall, C.; Lagatsky, A.A.; Sibbett, W.; Gunn-Moore, F.J.; Dholakia, K. *J. Biophotonics* **2008,** *1,* 183–199.
[89] Lei, M.; Xu, H.P.; Yang, H.; Yao, B.L. *J. Neurosci. Methods* **2008,** *174,* 215–218.
[90] Uchugonova, A.; König, K.; Bueckle, R.; Isemann, A.; Tempea, G. *Opt. Express* **2008,** *16,* 9357–9364.
[91] Yamaguchi, A.; Hosokawa, Y.; Louit, G.; Asahi, T.; Shukunami, C.; Hiraki, Y.; Masuhara, H. *Appl. Phys. A: Mater. Sci. Process.* **2008,** *93,* 39–43.
[92] Kohli, V.; Elezzabi, A.Y. *BMC Biotechnol.* **2008,** *8,* 7.

[93] Zeira, E.; Manevitch, A.; Khatchatouriants, A.; Pappo, O.; Hyam, E.; Darash-Yahana, M.; Tavor, E.; Honigman, A.; Lewis, A.; Galun, E. *Mol. Ther.* **2003,** *8,* 342–350.
[94] Samarendra, K.; Mohanty, M.S.a.P.K.G. *Biotechnol. Lett.* **2003,** *25,* 895–899.
[95] Hosokawa, Y.; Iguchi, S.; Yasukuni, R.; Hiraki, Y.; Shukunami, C.; Masuhara, H. *Appl. Surf. Sci.* **2009,** *255,* 9880–9884.
[96] Schinkel, H.; Jacobs, P.; Schillberg, S.; Wehner, M. *Biotechnol. Bioeng.* **2008,** *99,* 244–248.
[97] Paltauf, G.; Dyer, P.E. *Chem. Rev.* **2003,** *103,* 487–518.
[98] Vogel, A.; Noack, J.; Hüttman, G.; Paltauf, G. *Appl. Phys. B* **2005,** *81,* 1015–1047.
[99] Mori, K.; Gehlbach, P.; Ando, A.; Wahlin, K.; Gunther, V.; McVey, D.; Wei, L.; Campochiaro, P.A. *Invest. Ophthalmol. Visual Sci.* **2002,** *43,* 1610–1615.
[100] Gu, L.; Koymen, A.R.; Mohanty, S.K. *Sci. Rep.* **2014,** *4,* 5106.
[101] Levskaya, A.; Weiner, O.D.; Lim, W.A.; Voigt, C.A. *Nature* **2009,** *461,* 997–1001.
[102] Ohlendorf, R.; Vidavski, R.R.; Eldar, A.; Moffat, K.; Möglich, A. *J. Mol. Biol.* **2012,** *416,* 534–542.
[103] Christie, J.M.; Gawthorne, J.; Young, G.; Fraser, N.J.; Roe, A.J. *Mol. Plant* **2012,** *5,* 533–544.
[104] Conrad, K.S.; Manahan, C.C.; Crane, B.R. *Nat. Chem. Biol.* **2014,** *10,* 801–809.
[105] Wu, Y.I.; Frey, D.; Lungu, O.I.; Jaehrig, A.; Schlichting, I.; Kuhlman, B.; Hahn, K.M. *Nature* **2009,** *461,* 104–108.
[106] Strickland, D.; Lin, Y.; Wagner, E.; Hope, C.M.; Zayner, J.; Antoniou, C.; Sosnick, T.R.; Weiss, E.L.; Glotzer, M. *Nat. Methods* **2012,** *9,* 379–384.
[107] Mohanty, S.K.; Reinscheid, R.K.; Liu, X.; Okamura, N.; Krasieva, T.B.; Berns, M.W. *Biophys. J.* **2008,** *95,* 3916–3926.
[108] Packer, A.M.; Peterka, D.S.; Hirtz, J.J.; Prakash, R.; Deisseroth, K.; Yuste, R. *Nat. Methods* **2012,** *9*, 1202–1205.
[109] Papagiakoumou, E.; Anselmi, F.; Bègue, A.; de Sars, V.; Glückstad, J.; Isacoff, E.Y.; Emiliani, V. *Nat. Methods* **2010,** *7,* 848–854.
[110] Rickgauer, J.P.; Tank, D.W. *Proc. Natl. Acad. Sci. USA.* **2009,** *106,* 15025–15030.
[111] Andrasfalvy, B.K.; Zemelman, B.V.; Tang, J.Y.; Vaziri, A. *Proc. Natl. Acad. Sci. USA.* **2010,** *107,* 11981–11986.
[112] Papagiakoumou, E.; Anselmi, F.; Bègue, A.; de Sars, V.; Glückstad, J.; Isacoff, E.Y.; Emiliani, V. *Nat. Methods* **2010,** *7,* 848–854.
[113] Dhakal, K.; Gu, L.; Black, B.; Mohanty, S.K. *Opt. Lett.* **2013,** *38,* 1927–1929.
[114] Rickgauer, J.P.; Tank, D.W. *Proc. Natl. Acad. Sci. USA.* **2009,** *106,* 15025–15030.
[115] Yamaguchi, S.; Tahara, T. *Chem. Phys. Lett.* **2003,** *376,* 237–243.
[116] Vivas, M.G.; Silva, D.L.; Misoguti, L.; Zaleśny, R.; Bartkowiak, W.; Mendonca, C.R. *J. Phys. Chem. A* **2010,** *114,* 3466–3470.
[117] Dhakal, K.; Gu, L.; Shivalingaiah, S.; Dennis, T.; Morris-Bobzean, S.; Li, T.; Perrotti, L.I.; Mohanty, S. *PLoS One* **2014,** *9*, e111488.
[118] Mohanty, S.K.; Mohanty, K.S.; Berns, M.W. *J. Biomed. Opt.* **2008,** 13*,* 054049.
[119] Fu, L.; Jain, A.; Xie, H.K.; Cranfield, C.; Gu, M. *Opt. Express* **2006,** *14,* 1027–1032.
[120] Cao, G.; Platisa, J.; Pieribone, V.A.; Raccuglia, D.; Kunst, M.; Nitabach, M.N. *Cell* **2013,** *154,* 904–913.
[121] Ji, G.; Feldman, M.E.; Deng, K.Y.; Greene, K.S.; Wilson, J.; Lee, J.C.; Johnston, R.C.; Rishniw, M.; Tallini, Y.; Zhang, J.; Wier, W.G.; Blaustein, M.P.; Xin, H.; Nakai, J.; Kotlikoff, M.I. *J. Biol. Chem.* **2004,** *279,* 21461–21468.
[122] Tallini, Y.N.; Ohkura, M.; Choi, B.R.; Ji, G.; Imoto, K.; Doran, R.; Lee, J.; Plan, P.; Wilson, J.; Xin, H.B.; Sanbe, A.; Gulick, J.; Mathai, J.; Robbins, J.; Salama, G.; Nakai, J.; Kotlikoff, M.I. *Proc. Natl. Acad. Sci. USA.* **2006,** *103,* 4753–4758.
[123] Tian, L.; Hires, S.A.; Mao, T.; Huber, D.; Chiappe, M.E.; Chalasani, S.H.; Petreanu, L.; Akerboom, J.; McKinney, S.A.; Schreiter, E.R.; Bargmann, C.I.; Jayaraman, V.; Svoboda, K.; Looger, L.L. *Nat. Methods* **2009,** *6,* 875–881.
[124] Choudhury, N.; Zhang, Z.; Zhao, F.; Gu, L.; Mohanty, S. *Visual, Image Process. Comput. Biomed.* **2012,** *1,* 2012004984.
[125] Adler, D.C.; Huber, R.; Fujimoto, J.G. *Opt. Lett.* **2007,** *32,* 626–628.
[126] Choma, M.A.; Ellerbee, A.K.; Yang, C.; Creazzo, T.L.; Izatt, J.A. *Opt. Lett.* **2005,** *30,* 1162–1164.
[127] Joo, C.; Akkin, T.; Cense, B.; Park, B.H.; de Boer, J.F. *Opt. Lett.* **2005,** *30,* 2131–2133.
[128] Joo, C.; Kim, K.H.; de Boer, J.F. *Opt. Lett.* **2007,** *32,* 623–625.
[129] Wang, R.K.; Nuttall, A.L. *J. Biomed. Opt.* **2010,** *15,* 056005–056009.